Subglacial Geomorphology of Mizuho Plateau and around Yamato Mountains, East Antarctica

Kunio OMOTO*

1 Introduction

The principal purpose of the field survey during the summer season in 1969–70 of the 10th Japanese Antarctic Research Expedition (JARE–10) was to make strain grid band by means of triangulation along 72°S between 43°E meridian and the Yamato Mountains ca. 250 km westward, to identify the accumulation or ablation rate and ice movement in the Mizuho Plateau and to clarify glacial and subglacial topography along the inland traverse route (Fig. 1). The results have been reported by Omoto (1970), Ando (1971), Yoshida and Ando (1971), Yoshida, Ageta and Yagi (1971), Yoshida, Ando, Omoto, Naruse and Ageta (1971), Kusunoki (1971), Ageta (1971 and 1972), Kikkawa (1972), and Ishida *et al.* (1972).

As the 14th party followed the same route and re-measured the strain grid band, the rate of accumulation or ablation and ice movement in horizontal and vertical scale at each station were revealed (Naruse *et al.*, 1975).

This paper intends to present the subglacial geomorphology of the Mizuho Plateau and around Yamato Mountains based on the results of radio echo-sounding the present author operated throughout the inland traverse.

2 Oversnow traverse and Observation

The inland traverse party of JARE-10, a 10-man team led by H. Ando, crossed approximately 1500 km on the Mizuho Plateau in 90 days. The party left Syowa Station on Nov. 1, 1969 and returned on Jan. 29, 1970. The organization of the party and the equipments are shown in Tables 1 and 2. The basic observations and surveys throughout oversnow traverse were carried out in the following way: Shape and amount of the ice sheet were analyzed by surface topography of the ice sheet determined by barometric altimetry and leveling (for A164–A001), thickness of the ice sheet measured by radio echo sounding and gravimetric method, and elevation of the bedrock surface was estimated with surface elevation and thickness of the ice sheet. Instruments and methods for observation are explained as following.

(1) Astrofix

Astronomic observations were made at S170, 240, A075, 001, an east nunatak

* The author was a member of the 10th and 14th Japanese Antarctic Research Expedition.

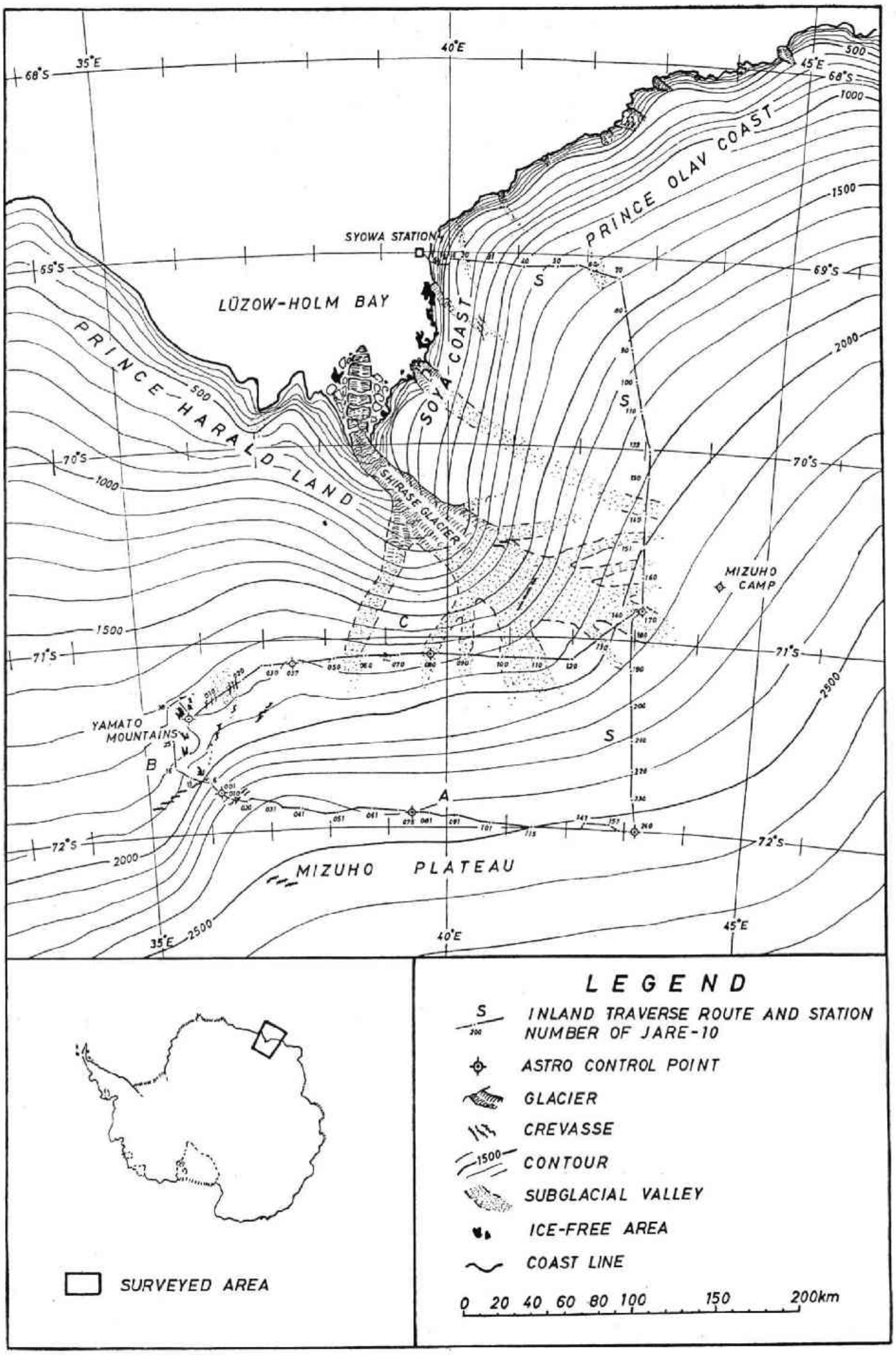

Fig. 1 Traverse route of JARE-10 and ice surface topography of Mizuho Plateau, East Antarctica (countour interval is 100 m).

Table 1. Members and Assignments of the inland traverse party of JARE–10

Name	Assignments
Hisao Ando	Leader, geology, seismic sounding
Masaru Yoshida	Geology, geomagnetism, gravity
Kunio Omoto	Geomorphology, barometric altimetry, geodetic survey, radio echo sounding, radio communication
Renji Naruse	Glaciology
Yutaka Ageta	Glaciology, meteorology, VLF, travel pilot
Masamoto Kikkawa	Medical doctor, radio communication
Shinpei Ishiwata	Chief mechanic
Minoru Yagi	Logistics, mechanic
Yuji Maeda	Mechanic, radio communication
Yukio Kimura	Press man of NHK, logistics

Table 2. Equipments of the inland traverse party of JARE–10

Oversnow vehicle	Transceivers
KD608, KD609 (Diesel engine) 2	JSB-31 (SSB, 2-14 Mhz, 50W)....2
KC2014, KC2015 (Gasoline engine) 2	EF-138 (VHF, 10W) 4
2-ton sledge 9	EK-118 (VHF, 1W) 2
caboose 1	FTDX-100 (SSB, 3.5-29Mhz, 50W) 1
Fuel	**Food**
Diesel oil ....6.0 kl Gasoline....................5.7 kl Kerosene ....0.4 kl	Food 2.0t

of D massif, C037 and 080 for determining geodetic positions throughout the traverse. Instruments were Wild T2-E theodolite with Roelofs eye-piece, FTDX–100 transceiver of special order to Yaesu Musen Co. for reception of world standard time, Seiko stopwatch 89ST same as used at Tokyo Olympiade, and a portable electric computer Canola 163 (Canon Business Machine Co.).

The author observed the sun with Wild T2-E theodolite hearing the standard time of WWV or WWVH at 10Mhz or 15Mhz. The results were computed at once with Canola 163 in snow car. The geodetic positions in this report were checked at the Geographical Institute, Ministry of Construction with NEAC-2206 Computer.

Average accuracy of the observations is 1.8″ in SDλ and 25.2″ in SDϕ. On the geodetic positions along the pole traverse route the values determined by JARE-9 (Fujiwara, Kakinuma and Yoshida 1971) were adopted, except S16 and 240. The geodetic position of S16 in this paper is located at slightly deviated position from that of the 9th, which was determined by JARE-11 by the traverse from an astro control point of Syowa Station. The geodetic positions from S240 to A002 were computed by triangulation chain from astro control point of A001, a southeastern nunatak of the Yamato Mountains. The other positions except around mountains were intercorporated between two neighbouring astro control points by navigation records.

(2) Altimetry

Altimetry is an important observation among other geophysical observations in the traverse, as the accurate altitude is expected. However precise leveling is hardly possible in limited time through the long traverse. A simple way to determine the surface elevation of ice sheet is the use of barometric altimeter. The 10th party used four barometric altimeters (American Paulin Altimeter, MM-1).

The altimeters were read every 2 km except along 72°S, where the altitude was determined by triangulation, by Mr. Naruse in KC2015 train and by the author in KD608 train. The author tried to correct the barometric errors by simultaneous reading at appointed time and interval. For this purpose, the readers 2 km apart, under the contact by radio in regular time interval, read each altimeter simultaneously five minutes after the arrival at each station. But the error of each instrument was not negligible, and the author had to apply "single altimeter method" at the arrangement of data. The readings of elevation difference between two neighbouring stations were averaged and corrected for air temperature. The route between S16 and S122 was travelled four times by JARE-10, and 11 each. And the route from S122 and 169 was travelled four times by the JARE-10 and three times by JARE-11. On the same route of the 10th and 11th, all the temperature corrected data were averaged again. The elevation of each station was calculated by accumulating the elevation differences successively onto the elevation of S16 (553 m a.s.l.).

The results of above altimetry are in good agreement with those by JARE-9 in general tendency, though there remained maximum disagreement of 58 m. The error of elevation for a closed circuit S170, 240, A003, B48 to S170 was 21m at S170. This might be due to the existence of polar anticyclone. Actually, the error was uniformly distributed over the closed circuit except between A164 and A003. The elevations of some peaks of the Yamato Mountains and other nunataks were determined by single method of altimetry and also by the triangulation from each camp sites at the Yamato Mountains, and expressed in later figure.

(3) Radio Echo-Sounding

During the inland traverse, radio echo-sounding, gravity measurement and seismic reflections were carried out to identify the thickness of ice sheet. MK-II radio echo-sounder of Scott Polar Research Institute, and SS-3101 TR-synchroscope of Iwasaki Comunication Co. were installed in the KD608 cabin (Figs. 2 and 3). They were spring-mounted in a cabin against the mechanical shocks due to uneven terrain as sastrugi zones (Fig. 4), but they were not thermostatically controlled and susceptible to low temperature as below −20°C, especially the radio echo-sounder. The electric power for the instruments was supplied from 12 volt battery of the KD608.

The transmitter emitted 500 watt peak pulse with repetition frequency of 15.625Khz at 32.5Mhz. For transmitting and receiving proper antenna was selected among folded dipole of 0.7 λ long, four-wire halfwave dipole and three elements Yagi beam, depending upon the condition of ice sheet. The dipole antenna was fixed to left side of the KD608 tractor (Fig. 2), while the Yagi beam was fixed on the first fuel sledge (Fig. 13). The output power and frequency was checked every day. A-scope echoes were read at every station and especially at every 500 m interval at the coast or near the mountains. The author calculated the thickness of ice sheet from the travel time of echoes using the electromagnetic wave velocity in ice sheet 171m/μsec after Clough and Bentley (1970). The results are expressed in Fig. 5 and Table 3, 4 and 5 (attached to the article end).

3 Subglacial Topography of Mizuho Plateau

The inland traverse route was divided into coastal, inland and around Yamato Mountains in convenience of explanation.

(1) Coastal Region

Coastal region is limited between St. Y1 and S80 about 120 km east of Syowa Station. Long-profiles of the ice surface and bedrock surface are expressed in Figs. 6 and 7. The ice surface increases it's height gradually and reaches 1473 m a.s.l. at S80, while the bedrock surface is nearly the mean sea level, with some exceptions. Two subglacial valleys between St. Y8 and 9, and between S19 and 20 are deeper than 500 m below mean sea level. Syowa Station is on East Ongul Island separated beyond 4 km wide strait, of which depth reaches more than 600 m below mean sea level (Fujiwara 1971). Subglacial rises are observed

Fig. 2 KD608 snow-car. Radio echo sounding antennas are fixed on both sides of snow-car.

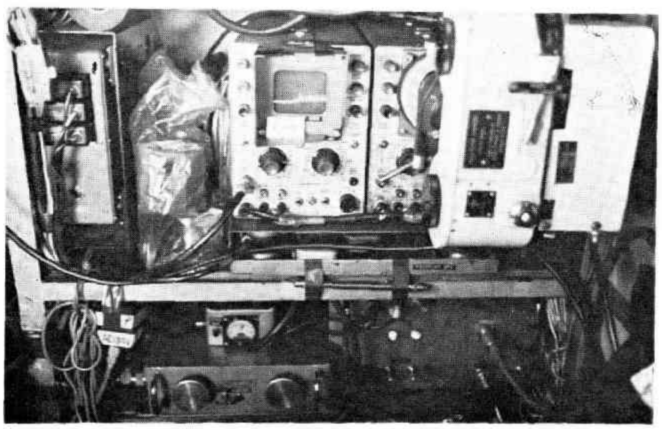

Fig. 3 Radio echo sounder mounted in KD608 cabin. Arrangement: Transmitter (lower right), Receiver (lower left), Camera for continuous echo sounding (upper right) and monitor CRO (upper left).

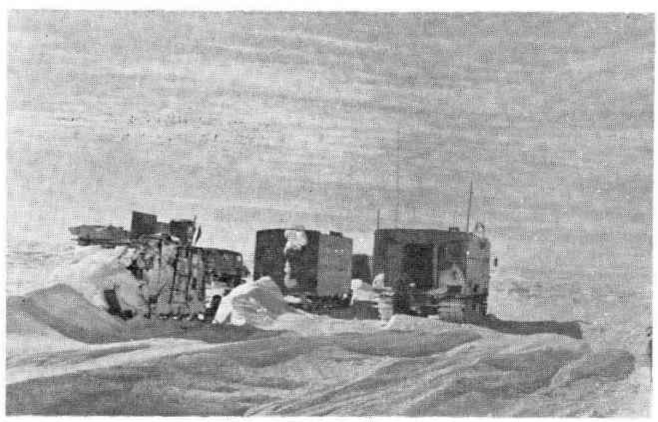

Fig. 4 Camp site near sastrugi zone.

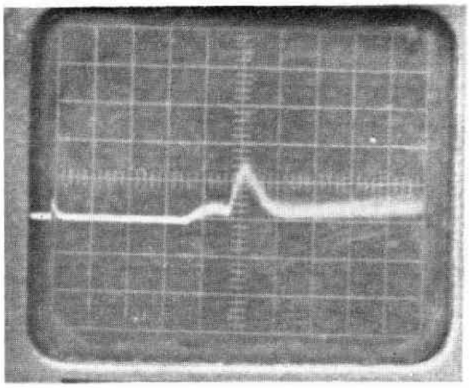

Fig. 5-1 S17-15-6.5

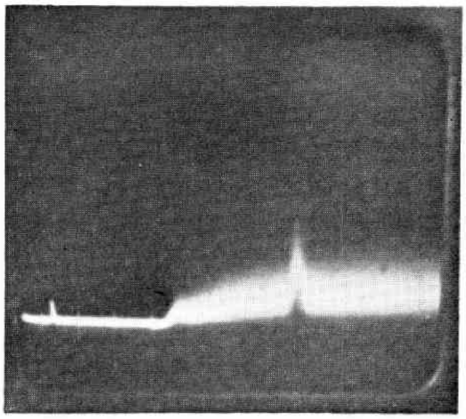

Fig. 5-2 S21-7-6.5

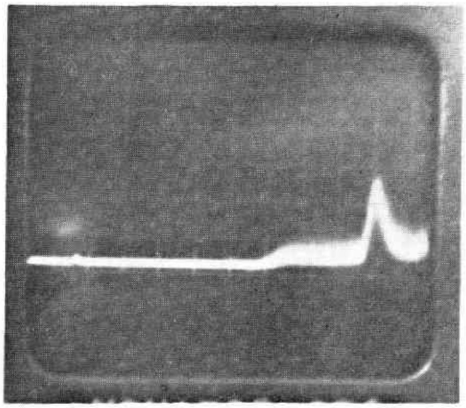

Fig. 5-3 S25-13-8.3

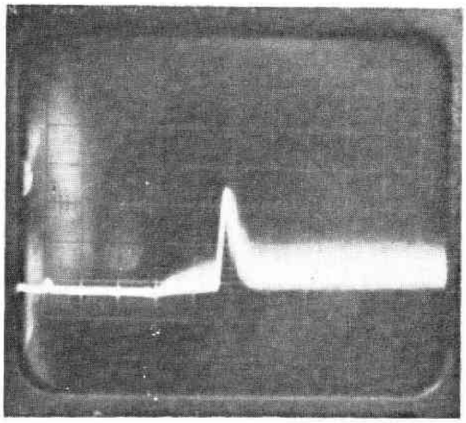

Fig. 5-4 S26-15-9.2/10.0

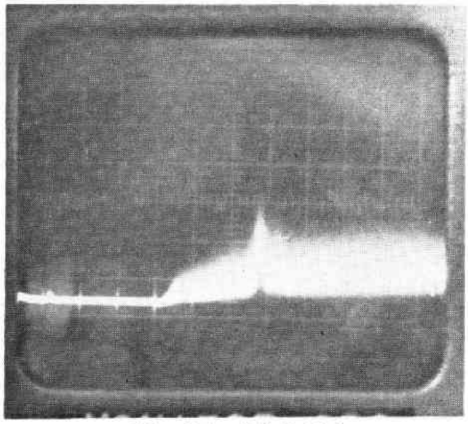

Fig. 5-5 S28-5-11.0

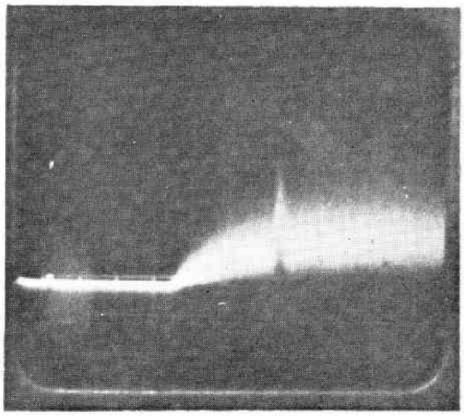

Fig. 5-6 S36-0-12.3

Fig. 5 Selected A-scope echoes. The first group of number means figure number, the second group indicates station number, the third group indicates attenuation of the receiver in dB, and the last group indicates travel time in μ sec.

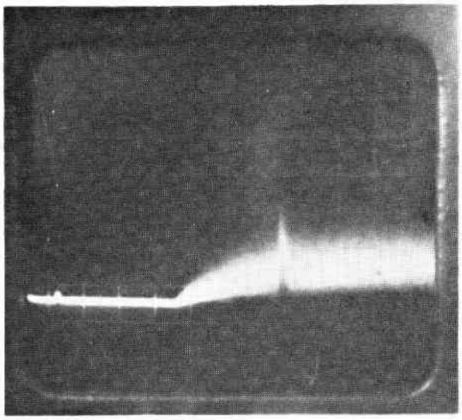

Fig. 5-7 S38-1-12.9

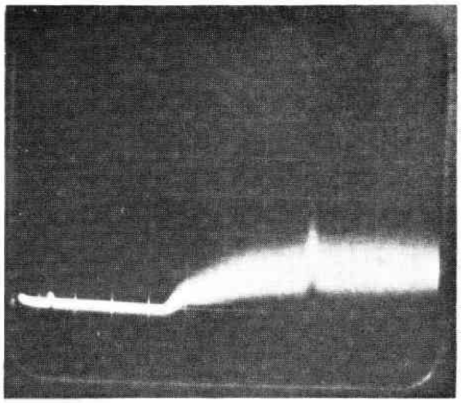

Fig. 5-8 S48-0-14.5

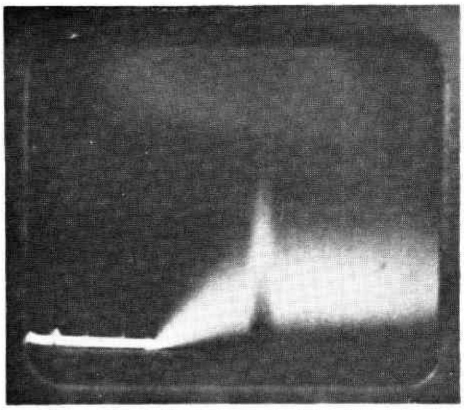

Fig. 5-9 S58-2-11.5/12.8/13.9/14.6

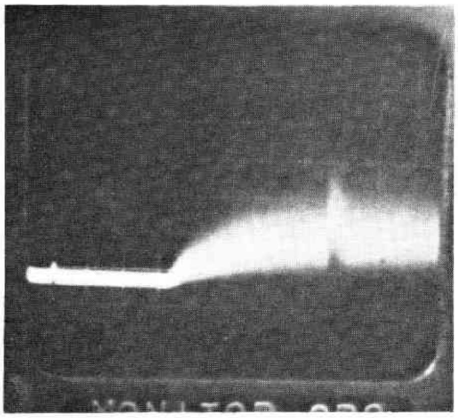

Fig. 5-10 S60-0-15.5

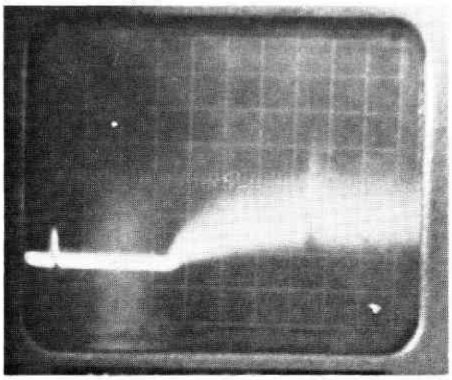

Fig. 5-11 S68-3-14.75

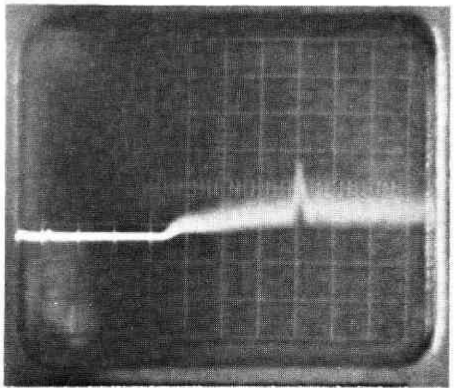

Fig. 5-12 S110-5-14.35

Fig. 5 (continued)

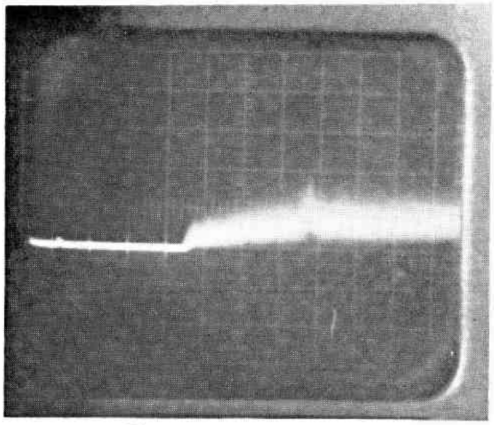

Fig. 5-13 S116-4-13.45

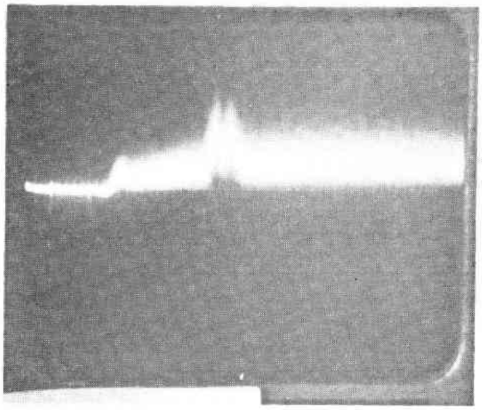

Fig. 5-14 A016 (2.5 km to the east point)-35-8.70/9.30

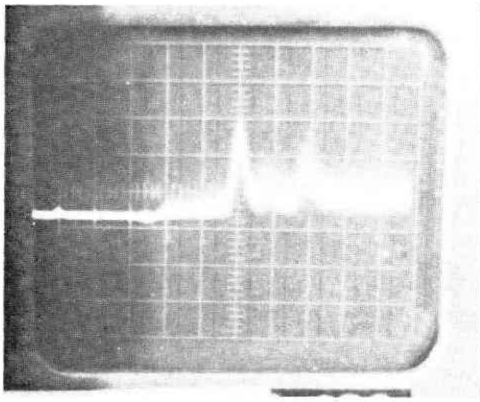

Fig. 5-15 A004-43-5.00/6.95

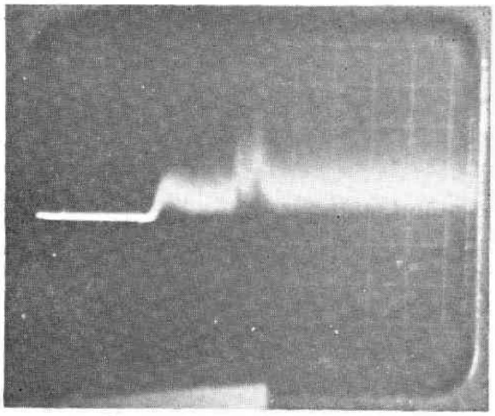

Fig. 5-16 B5-18-9.40/10.40

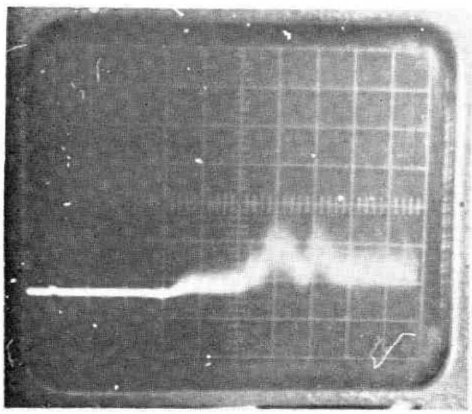

Fig. 5-17 B9-40-6.20/7.25

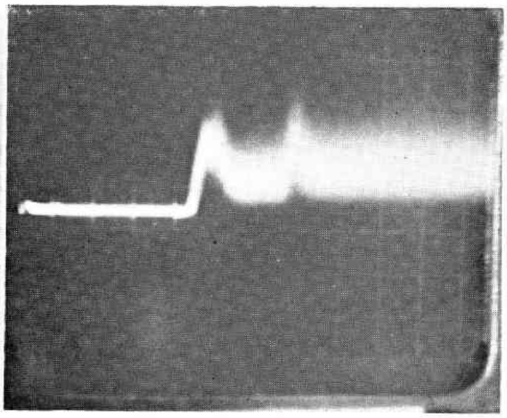

Fig. 5-18 B18-6-11.45

Fig. 5 (continued)

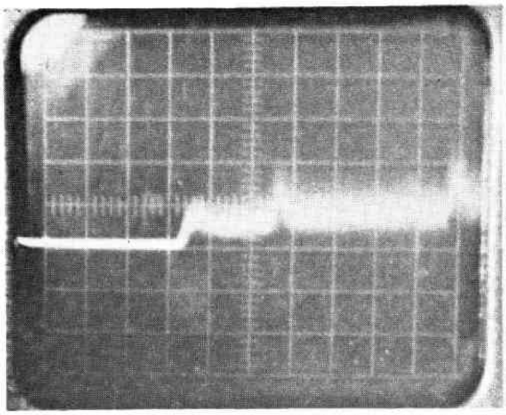

Fig. 5-19 B19-11-10.40/17.66/19.94/20.06/20.18

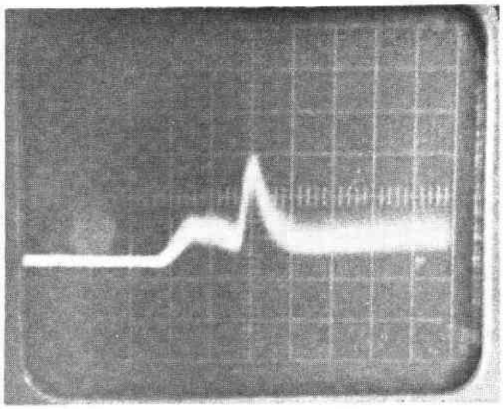

Fig. 5-20 B25-46-5.00

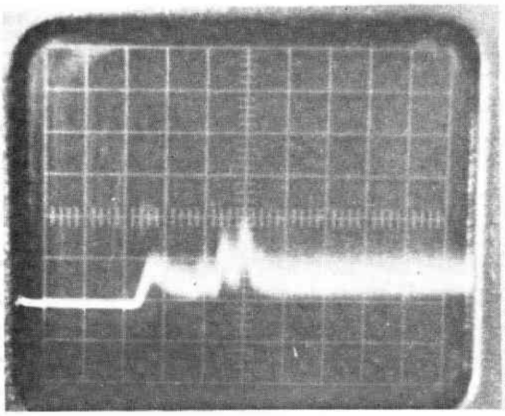

Fig. 5-21 B31-20-8.00/9.00/10.08

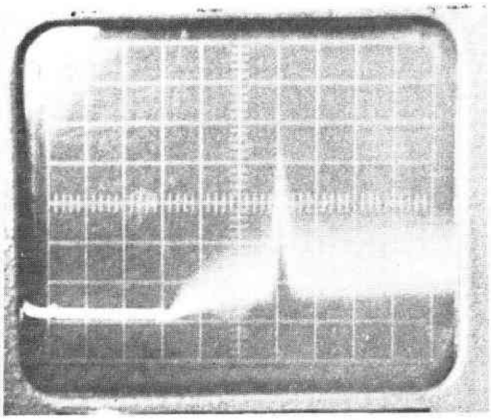

Fig. 5-22 B32-18-12.12

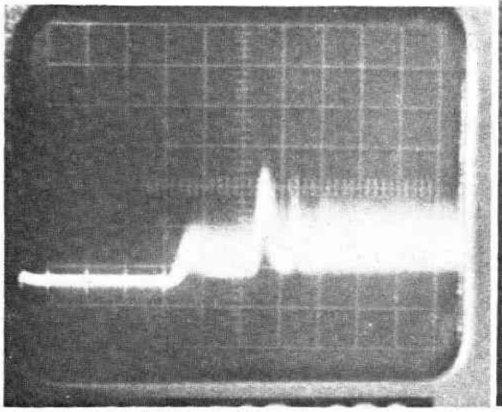

Fig. 5-23 B33-10-11.20/12.64/14.10

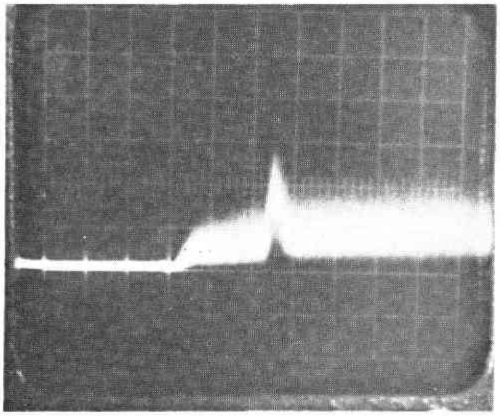

Fig. 5-24 B36-14-11.28

Fig. 5 (continued)

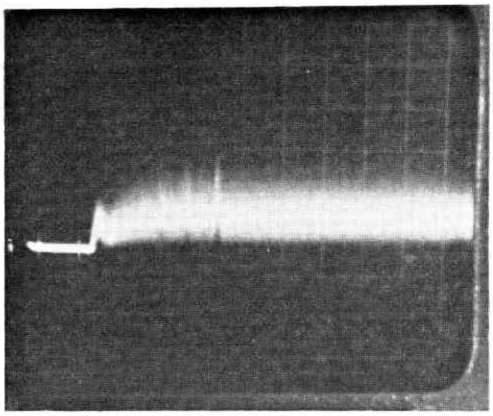

Fig. 5-25 B46-8-15.75/18.80/20.40/22.23

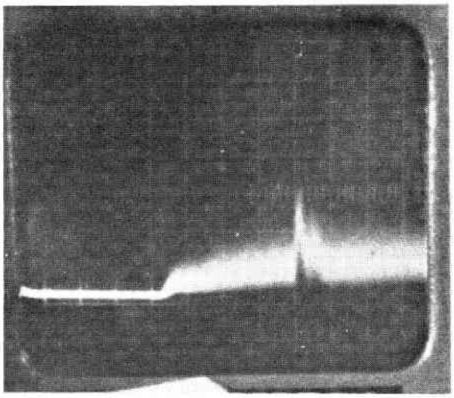

Fig. 5-26 C012-14-14.30/15.00

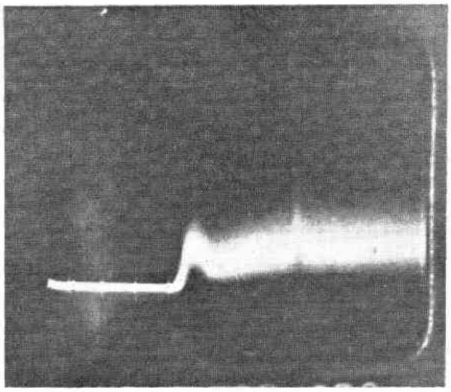

Fig. 5-27 CC023-3-13.70

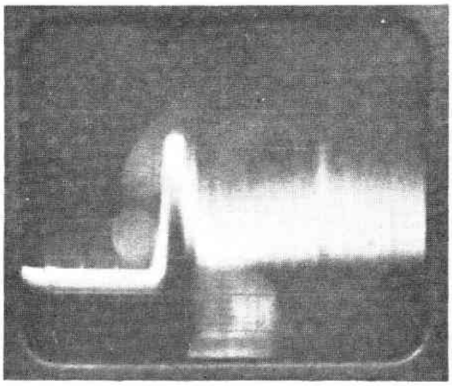

Fig. 5-28 C039-1-5.65/17.00

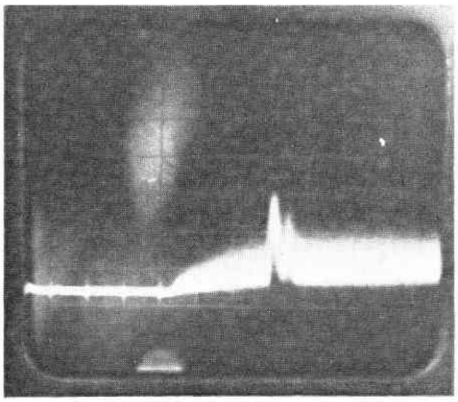

Fig. 5-29 C044-13-12.32/13.00

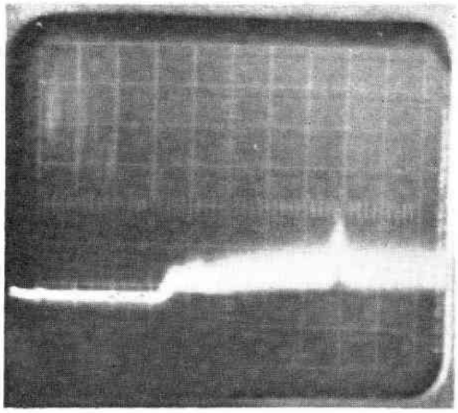

Fig. 5-30 C047-3-16.00

Fig 5. (continued)

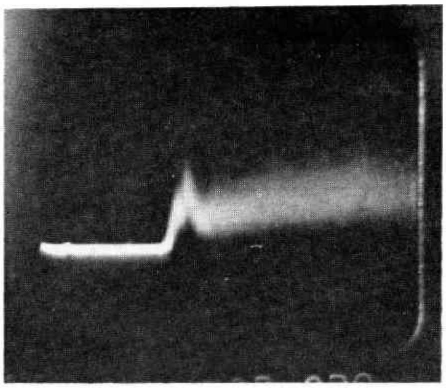

Fig. 5-31 C050-?-16.30

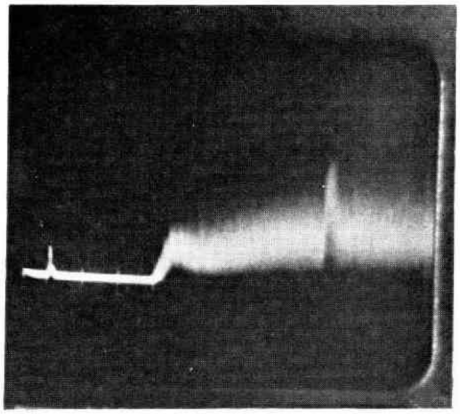

Fig. 5-32 C068-1-16.00/17.30

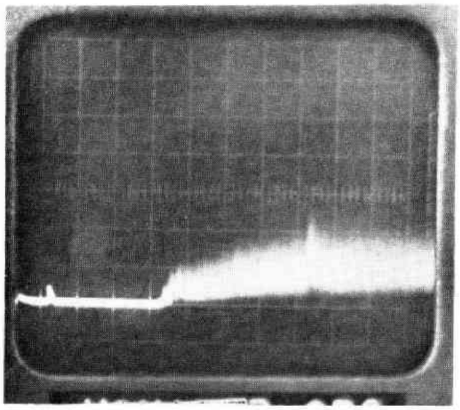

Fig. 5-33 C074-6-14.75

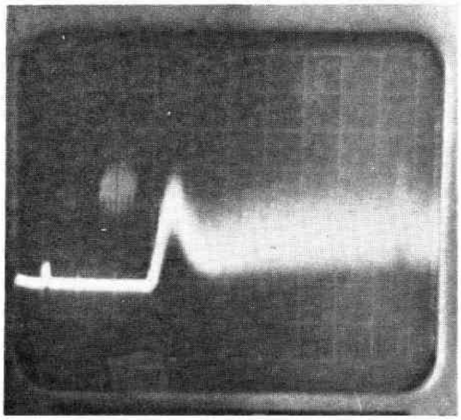

Fig. 5-34 C084-0-19.47

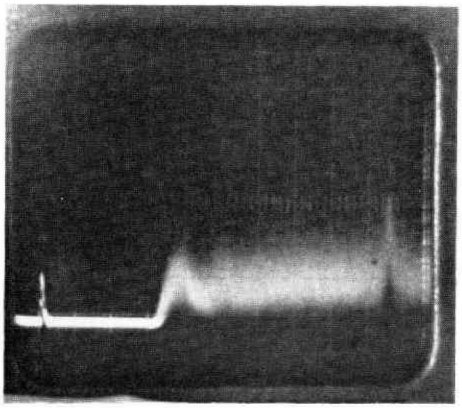

Fig. 5-35 C093-3-19.33

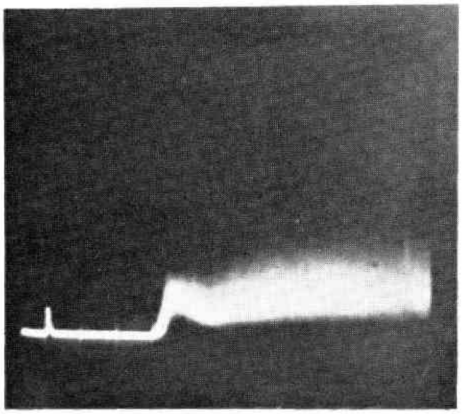

Fig. 5-36 C108-0-20.60

Fig. 5 (continued)

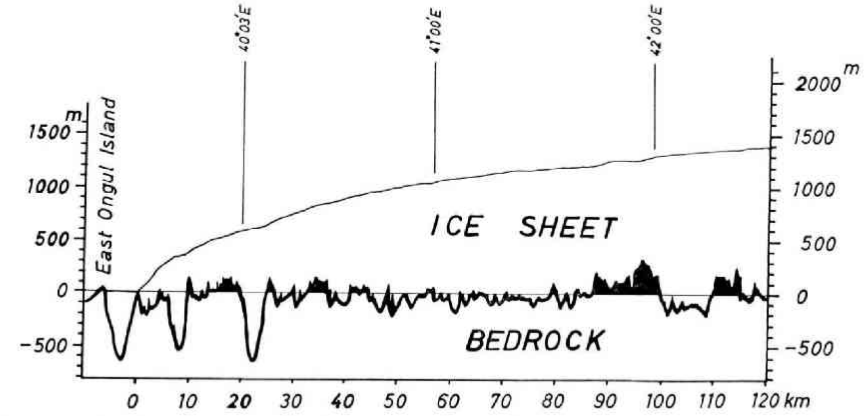

Fig. 6 Subglacial topography between station Y-1 and St. 70, east of Syowa Station

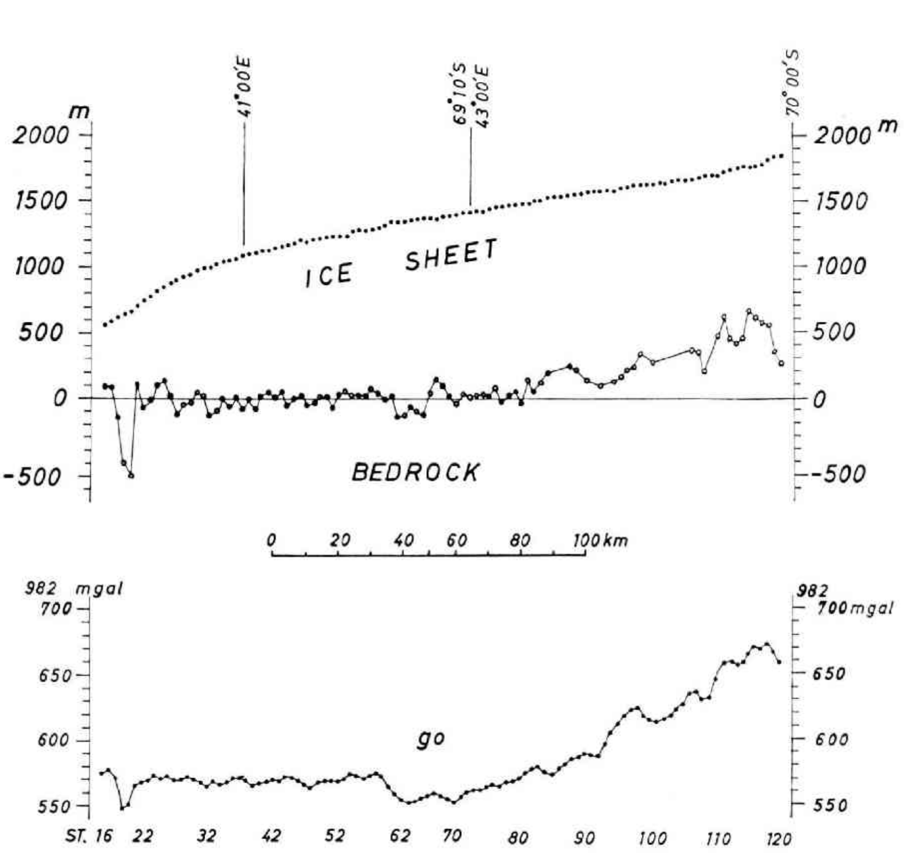

Fig. 7 Subglacial topography between St. 16 and St. 120 and changes of "go" values (gravity)

between S57 and 59, and between S65 and 68 about 300 m above neighbouring stations. Gravity values agree well with the data of radio echo-sounding in this region. Continuous bottom echoes are shown in Figs. 8 and 9 showing smooth bedrock surface against complicated bedrock surface of Figs. 6 and 7.

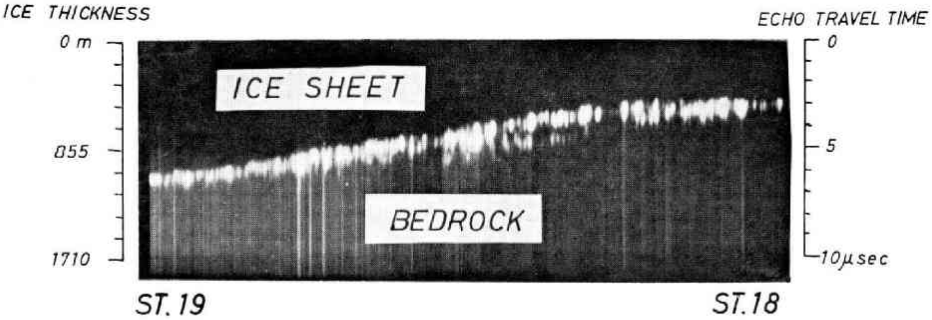

Fig. 8 Continuous bottom echoes between St. 18 and 19

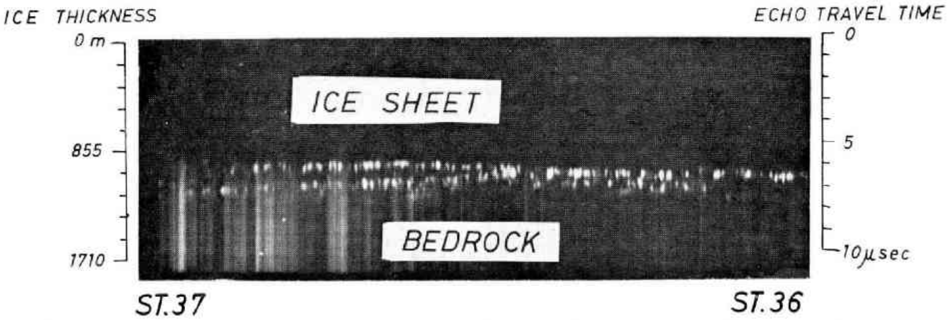

Fig. 9 Continuous bottom echoes between St. 36 and 37, where multi-echoes observed

(2) Inland Region

Inland region is limited here by the traverse route of the 10th; the route along the meridian of 43°E, and two routes along 72°S and 71°S between 43°E and Yamato Mountains. In this region, the ice surface elevation agree very well with the changes of the gravimetric values between S80 and 160. The bedrock elevation increases gradually southward, with big fall at S92, 120, 142, 158, 169 and with small fall at S80, 100, 108, 113, 126. The value of "go" (gravity value reduced to sea level by free air reduction) increases gradually (Fig. 10), with large drop at S101, 120, 133, 147, 160, medium drop at S85, 108, 130, 184, 200, 207, and small drop at S91, 174, 177. A deep and broad subglacial valley or basin is found between S127 and 173, while a subglacial rise or mountain is observed between S92 and 147.

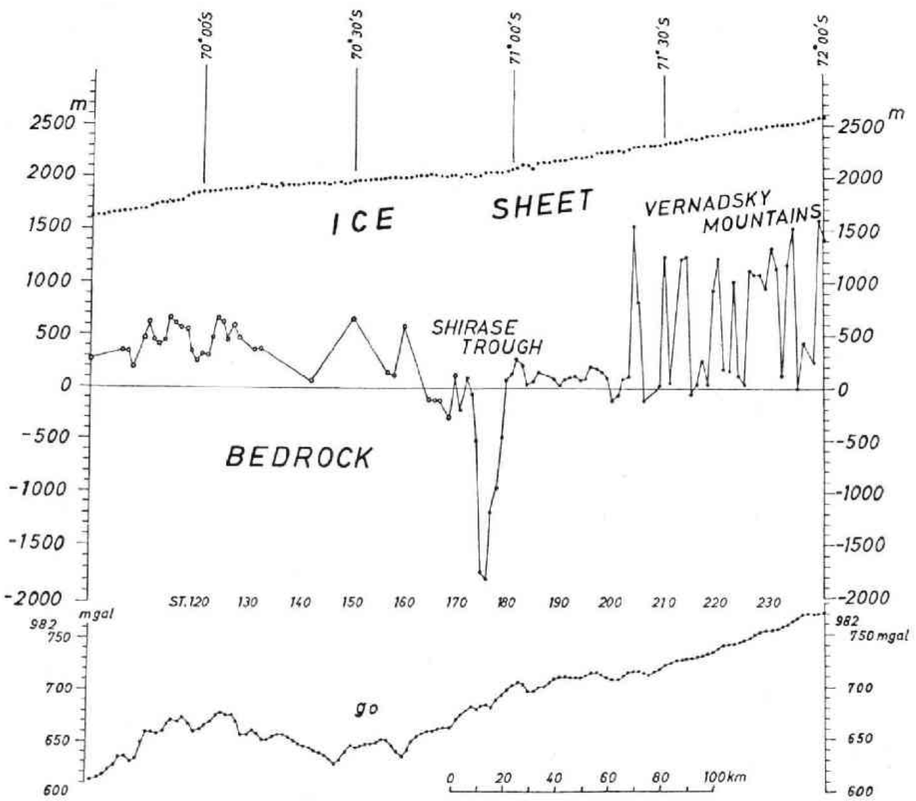

Fig. 10 Subglacial topography along the meridian of 43°E and changes of "go" values (○ was sounded by JARE-10, while ● was sounded by JARE-14)

Judging from the radio echo-sounding and gravity data, two deep subglacial valleys are expected at S147 and 160, although the echo obtained is not clear. From S170 the gravity value increases monotonously except S174, 177, 184, 200 and 207, while the radio echo-sounding show rather complicated subglacial topography. The bedrock elevation agrees well with the gravity data between S170 and 203, but greatly disaccords at other stations. A conspicuous subglacial valley 1800m deep below mean sea level or about 2000m deep below the neighbouring stations was sounded at S176, or between S172 and 182. A conspicuous subglacial mountain rising 1500m above surrounding bedrock surface was found southward from S204.

Apart from meridian of 43°E, complicated subglacial feature is getting monotonous and harmonic with the gravimetric data (Fig. 11). The subglacial mountains observed along the meridian of 43°E are no more found at A109.

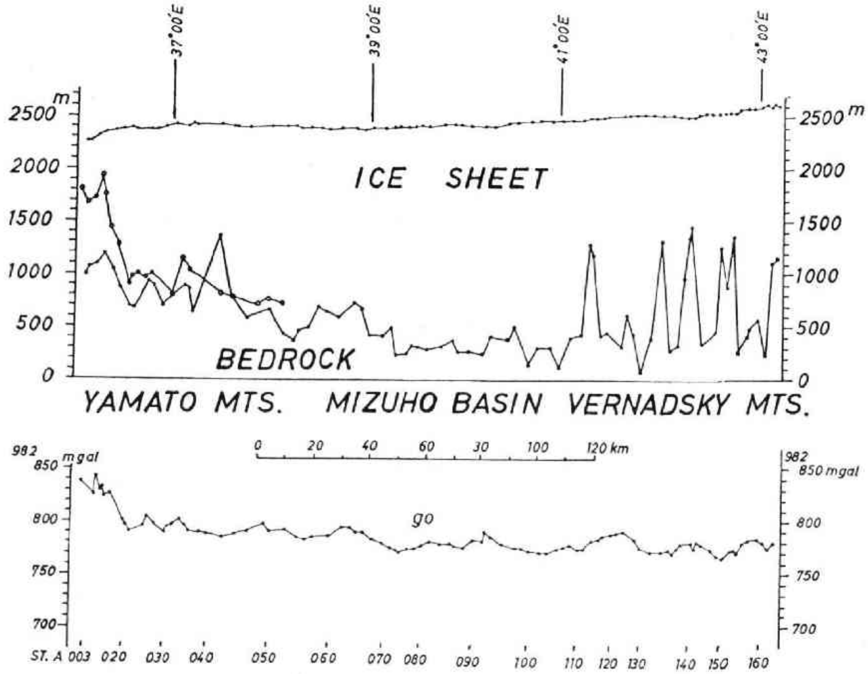

Fig. 11 Subglacial topography along 72°S and changes of "go" values

Subglacial mountain peaks complicated in feature are detected 1200m below the ice surface (1200 m–1500 m a.s.l.), whose relative heights are ca. 1000 m. The subglacial bedrock surface is comparatively monotonous from A109 to A003 and gradually elevating toward Yamato Mountains. The bedrock relief is less than 500 m in relative height except A041, and has no conspicuous depression or eminence. The gravity data are correspondent with the radio echo-sounding data except between S240 and A109. Some differences between both data and between those of the 10th and the 14th are perhaps caused by the locational difference of measuring site.

The surface of ice sheet along 71°S is about 1800 m a.s.l. in height for 100 km long from the east of Yamato Mountains to C050, then it increases the height gradually and reaches 2000m a.s.l. at S170 (Fig. 12). The ice surface topography matches well to the subglacial topography. The ice surface topography, bedrock surface and "go" values of the gravity are shown in Fig. 12, in which the subglacial topography along 71°S is apparently complicated. The discordant values between the radio echo-sounding and gravity are recorded at C013, 026, 089, 115, 126, and other stations. The gravity data are slowly changing and falling at C009, 021, 026, 060, 089, 102, 116, 124, and 129, while rising at C002, 014, 035–46,

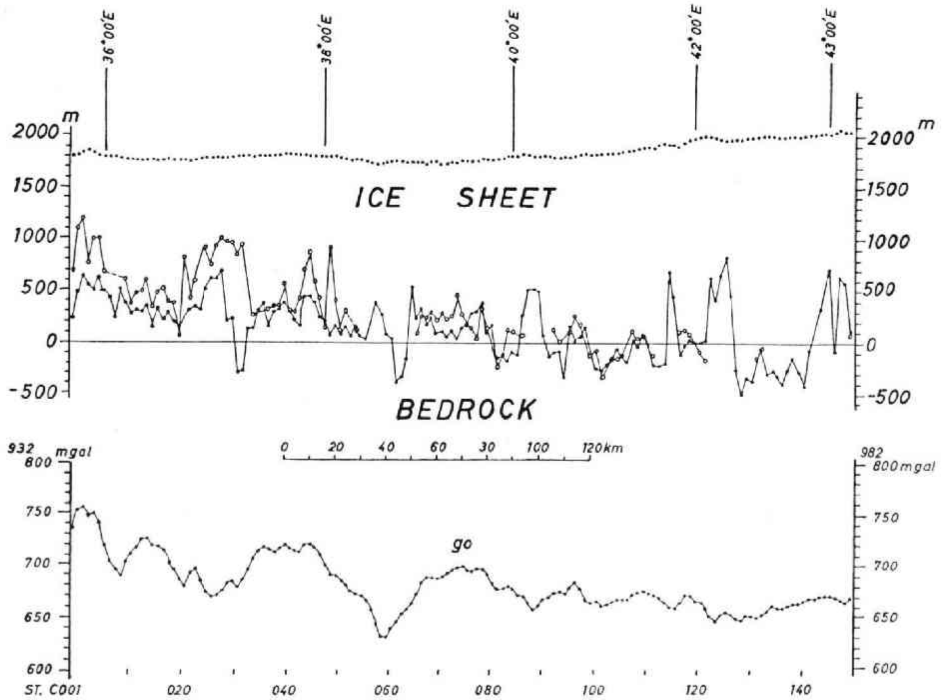

Fig. 12 Subglacial topography along 71°S and changes of "go" values

068–080, 097, 110, 118, and 146. The bedrock surface by the radio echo-sounding is complex and shows complicated subglacial topography with several deep valleys and mountains of several hundreds meters in relative height. Narrow subglacial valleys are observed at C030–033, and 060–065, and wider at C080–088, 090–096, 100–108, 110–115, 116–123, and 126–146. Deep and broad valley or basin are observed between C126–146, 116–123, 90–115, 079–088, 065–079, 046–058, and 009–026. The sudden rise of bedrock surface at the east of C115 suggests subglacial mountains about 1000 m in relative height.

(3) Around Yamato Mountains

The inland ice is descending gradually from A010 at the east of Yamato Mountains to B13 at the west. The ice surface is 2338 m a.s.l. in height at A010 and 1933m a.s.l. at B13 i.e. the difference in elevation between the east side and the west side of the mountains reaches about 400m. The kind of ice is bare ice or blue ice around the Yamato Mountains always under katabatic wind from the east. Blue ice was exposed widely at the west of the mountains except closer to the massif. The ice surface descends northward to 1630 m a.s.l. at B41 at the west side of the mountains. The route from B41 to 48 climbs the outlet glacier between E and D massifs, and the ice surface ascends gradually up to 1800 m a.s.l.

Subglacial topography around Yamato Mountains differs from that of inland. The bedrock surface is comparatively low in relief and basin-like in structure far at the east of the mountains, but it gradually rises from 1909 m a.s.l. at A020 to 1948m a.s.l. at A010. The flat plateau-like ice surface changes into steeply inclined downslope at A014, whereabout appeared many wide crevasses covered mostly with snow as snow-bridges. This ice surface change was a reflection of the subglacial bedrock surface change such as the subglacial rise below A010 and gradual descending around. Other rises at A003 or B1 are explained by two nunataks "Mika" and "Sachiko" (temporary names) near A003 or B1, i.e. these nunataks made bedrock rise. The bedrock surface descends once from there, and ascends again to the foot of the Yamato Mountains.

Yamato Mountains were surveyed by JARE-4, 5 and 8 previously and reported by Yoshida (1961), Kizaki (1961), Yoshida and Fujiwara (1963), and Fujiwara (1964) on geology and geomorphology, i.e. the Yamato Mountains, located at about 200 km south of Prince Harald Coast, East Antarctica, extend about 50 km from north to south an arcuate chain, comprising seven massifs temporarily named A,B,C,D,E,F and G from south to north (Figs. 13–22). They consist of various gneisses, plutonics, metabasite and pegmatite which belong to a plutonic complex. These metamorphics and plutonics suffered strong foliation with strikes N 0°–20°E and dips about 20°–50° eastward. The rock is identified of each massif; A: charnockitic gneiss, diorite, biotitediorite, B: metabasite, augengneiss (partially rapakivi), granite-gneiss, granite, pegmatite, C: plagioclase porphyritic diorite, granite, pegmatite, D: metabasite, biotite-quartz diorite, granite-gneiss, pegmatite, E and F: granite-gneiss, G: injection gneiss.

The massifs are glaciated by the inland ice or the mountain glaciers under strong control of geological structure and they are separated by outlet glaciers. The inland ice varies 200 m to 400 m in height between both sides of the mountains, and the outlet glaciers descend gently across the mountains. The inland ice flows from ESE to WNW at the east of the mountains, which are acting as hinderance. Thus, the inland ice forms there plateau-like flat surface, which may be suggested by radio echo-soundings. On the east side of the mountains, snow is accumulating but on the west in the lee ablation is evidenced such as moraine banks or precipitous glaciated mountain flanks.

Recent deglaciation is proved everywhere in the mountains by vacant glacial throughs, cirques, shrinked cirque glaciers, isolated moraines, dead ice covered

Fig. 13 Inland traverse party near nunatak "Mika" southeast of Yamato Mts.

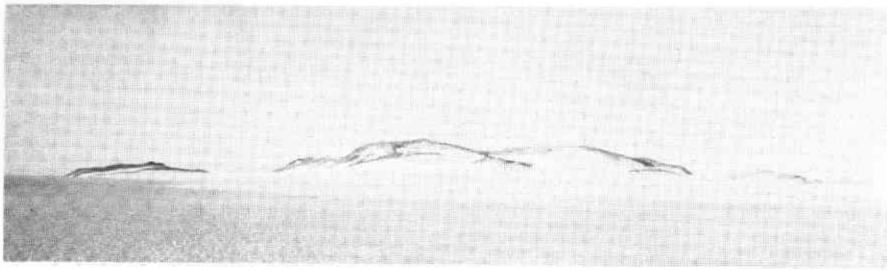

Fig. 14 Southeastern view of A massif of Yamato Mountains

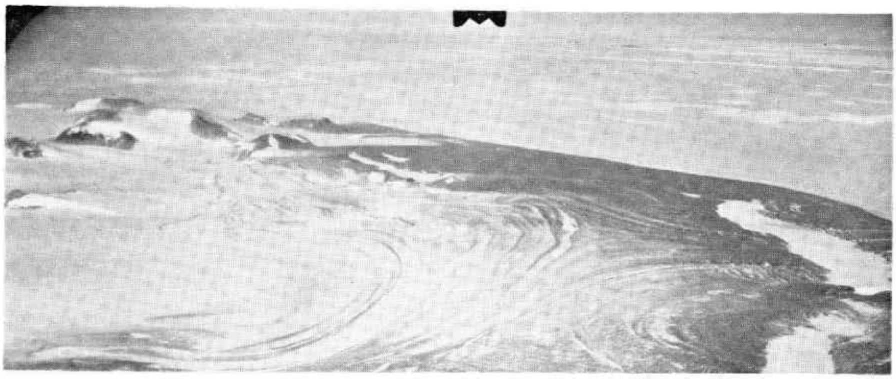

Fig. 15 A massif and northern moraine viewed from air

with moraines, and so on. These landforms tell that the shrinkage of glaciers have been gradually propagated from north to south.

The subglacial topography along the radio echo-sounding route at the west of Yamato Mountains evidenced the geological structure of the mountains. The subglacial rises are interpreted as the westward extensions of the massifs (Fig. 23). The subglacial depressions between rises are strongly scooped bedrocks by outlet glaciers. There are subglacial rises at B31 and B42. The sounding along the outlet glacier between D and E massifs resulted in the longitudinal section

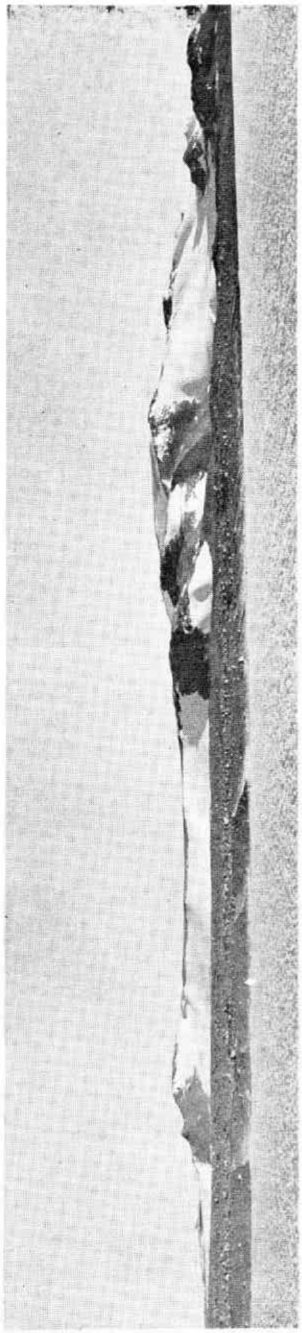

Fig. 16 A massif and moraine bank viewed from west

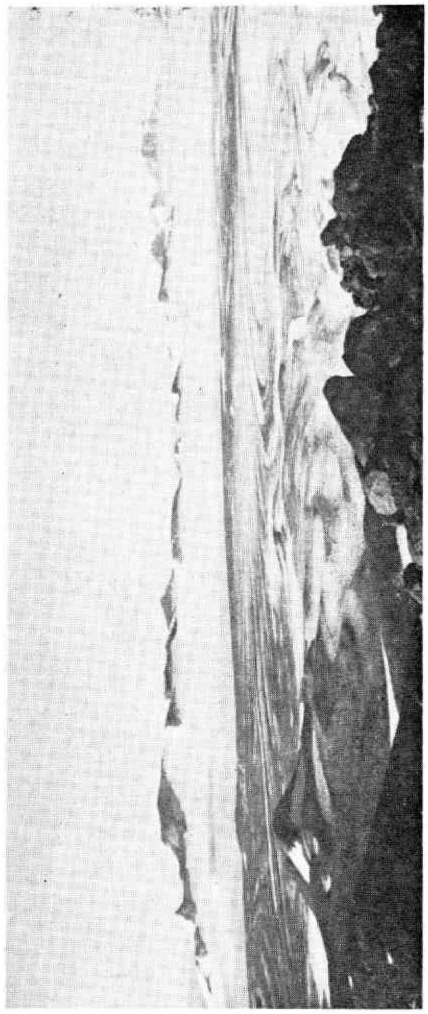

Fig. 17 B massif at middle left, C massif at middle center and D massif at middle right, and moraine on ice between A and B massifs viewed from 2380 peak of A massif

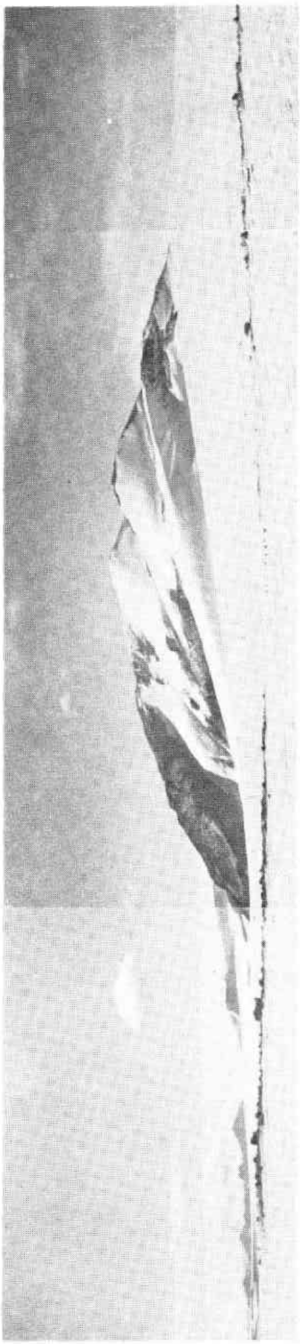

Fig. 18 B massif at center, an outlet glacier between A and B massifs at right, and C massif and an outlet glacier between B and C massifs at left, viewed from southwest of B massif

Fig. 19 Inland traverse party at base camp at the west of D massif of Yamato Mountains

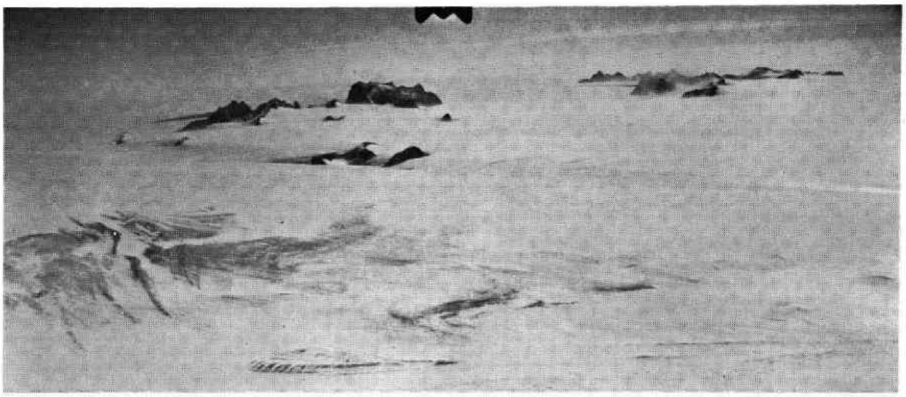

Fig. 20 D massif at upper left, moraine on ice and outlet glaciers between E, F and G massifs at upper right viewed from air

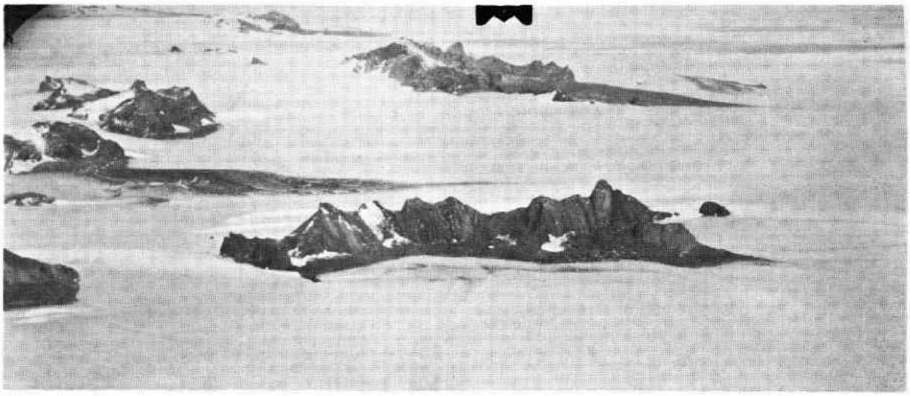

Fig. 21 B and C massifs at upper left, D massif at upper middle, E and F massifs at middle left, G massif and moraine on ice at center (Oblique view from air)

between B43 and 48 in Figure 23, which shows the outlet glacier reaching nearly 2000 m in depth and scooping out bedrocks deeply. The subglacial rises between B48 and C005 are the eastward extension of E massif. The bedrock surface descends gradually from C005 and becomes undulated. The gravity measured around Yamato Mountains agrees well with the echo-sounded data as shown in Fig. 23.

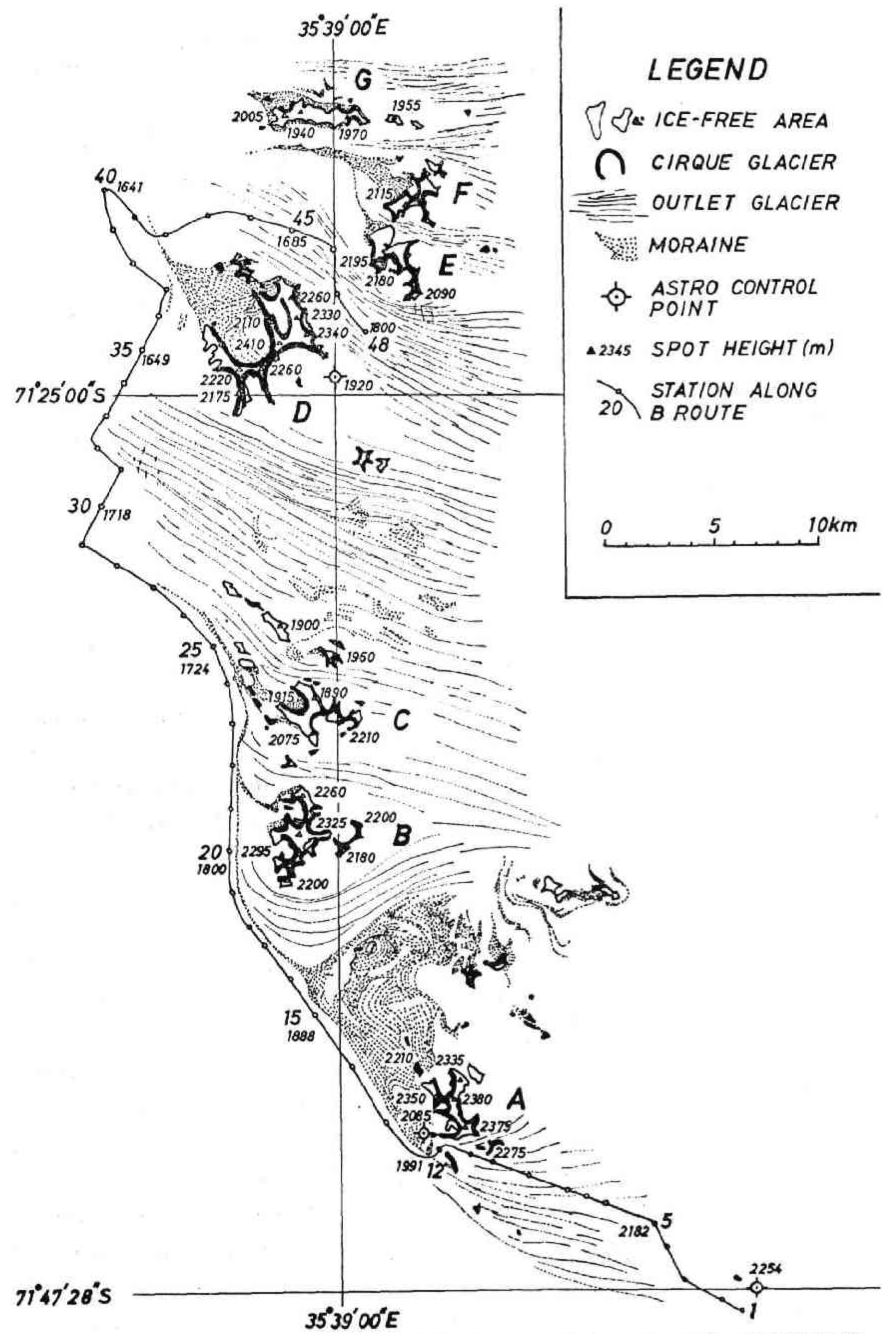

Fig. 22 Geomorphic map of Yamato Mountains and traverse route of JARE-10

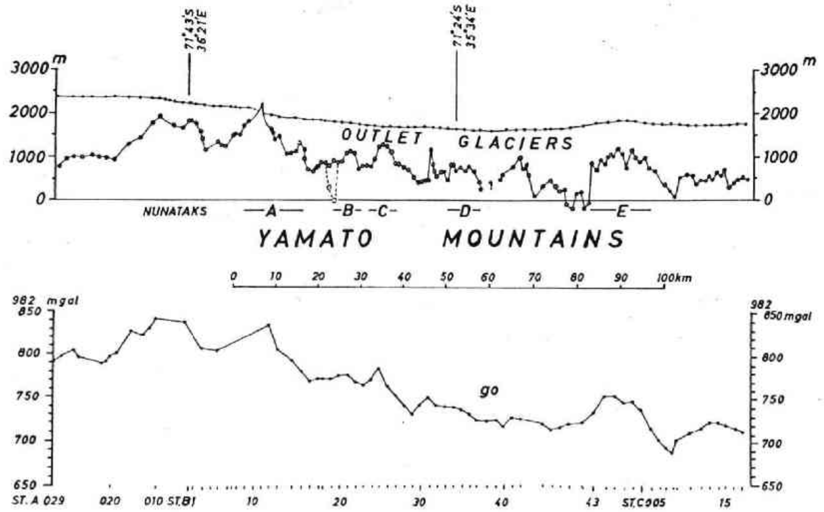

Fig. 23 Subglacial topography around Yamato mountains (sounding route is shown in Fig. 22)

4 Discussion

(1) Accuracy of altimetry and echo-sounding

Prior to morphological discussion, it is necessary to examine the error of altimetry and echo-sounding.

As for the error of ice surface altitude, there was 21 m of error for a closed circuit about 700 km in total distance through S170 via S240, A003, B48 to S170. Excluding the route between S240 and A003, whose elevation had been determined by triangulation, the reduced distance is 460 km i.e. the error is less than 5 cm/km. Thus the accuracy of altimetry seems to be satisfactory for the following discussion.

As for the error of the radio echo-sounding, the value of 171 m/μsec as electromagnetic wave velocity in ice sheet the present author used in this paper after Clough and Bentley (1970) should be examined. It is said to be valid for the temperature of −10°C below 10 m from the ice surface. Otherwise, Yoshino and Eto (1971) adopted the value of 169 m/μsec at the pole traverse of JARE–9. The velocity difference of 2 m/μsec means the error about 20 m per 1000 m ice thickenss. The accuracy of the radio echo-sounder is also to be mentioned. According to Evans (1963), the error of ice thickness measured by SPRI MK–1 estimated to be ±5 m, and Drewry (1972) reported that MK–IV system of S.P.R.I operated at 35 MHz and ranged in ice to an acuracy of 10 m could be resolved. Therefore, the error by MK-II radio echo-sounder the author used may be in the same order.

Reliability of reading the travel time on CR-oscilloscope, especially in the case of multi-echoes, will be commented later.

Concluding the above errors on both altitude and ice thickness, the measuring accuracy seems to be sufficient for discussion unless the absolute height of bedrock surface is treated in order of a meter. Generally speaking, the discussion should be in order of 10 m as lower limit, and the possible errors hardly exceed 50 m at maximum.

(2) Analysis of multi-echoes and comparison with gravimetric method, in determination of the ice thickness

Multi-echoes observed in many stations are troublesome to determine the true ice thickness above bedrock (Tables 3, 4, 5 and Figs. 5–4, 5–9, 5–14, 5–15, 5–16, 5–17, 5–19, 5–21, 5–23, 5–25, 5–26, 5–28, 5–29 and 5–32). The strongest echo or the first echo would be the true echo from the bottom. But they might be the echo from moraines among ice sheet. The multi-reflected echoes could be distinguished from return pulse with attenuated height and rounded shape. The author adopted the average travel time and the group wave velocity, and distinguished the echoes from the bottom with the continuity to the neighbour, obtained from the record of blightness modulation on CR-oscilloscope. Following alternation is considered on the multi-peaked echoes (Figs. 5–4, –9, –14, –16, –17, –19, –21, –23, –25, –26, –28, –29 and –32), i.e. uneven layer in density such as moraine layer or irregular bottom surface. The emitting beam of the radio echo-sounder is not so sharp as a line.

It was a remarkable and unsolvable problem for the author that some spans were not sensible to echo from the bottom, especially between S170 and 240, between S240 and A051, and between C123 and 170. Fortunately the 14th party caught the echo on the same spans, and the present author could discuss the subglacial topography through the route.

The bottom topography inferred from the echo obtainad by the 14th party is thought to be more complicated than expected, especially between S203 and 240, between A163 and A109, and at other spans. In order to solve the inconsistency, the sound results by the 14th and the 10th parties and the gravimetric data of the 10th party are compared.

According to Figs. 11 and 12, their reliefs have obviously of same tendency with some exceptions. The depth of the 14th is, in general, deeper than that of the 10th. Lacking echo of the 10th party is impossible to be compared with the corresponding data of the 14th party, but it is possible to check the echo of the 14th party with the gravimetric data of the 10th party instead of the echo of the 10th party. The gravity data are obviously of the bedrock surface at the place of negligible Bouguer anomaly (Figs. 7, 10, 11, 12 and 23). Comparing the echo data of the

14th party with the gravimetric data of the 10th, subglacial relief is more complicated in the former than in the latter, especially at the spans between S203 and 240, between A163 and A109, and others. There were found reliefs in opposite sense at some places; the echo shows convex subglacial topography and the gravimetric data at the same place concave one, *vice versa*. If the gravimetric data are correctly showing the concave, the convex relief of the echo data may be caused by misreading on the CR-oscilloscope or by the imbedded layer in ice sheet. If the gravimetric data are showing the convex, the concave relief of the echo is true, unless it is not multi-reflected and the gravimetric data is effected by Bouguer anomaly.

(3) Subglacial Topography

The ice surface topography in the coastal region was reported to be "marginal slope" by Fujiwara (1964) and Fujiwara *et al.* (1971). In this region, the ice surface ascends rapidly and becomes gentler inland. The cross or longitudinal profiles of ice sheet resembles well to hypsographic curve of the ice Antarctica given by Meinardus (1926), and to parabolic form given by Bardin and Suyetova (1967).

To the east of Syowa Station, there are three deep valleys whose depth exceed 500 m below mean sea level. One of them is a submarine valley situated in Ongul Strait, whose feature was described by Fujiwara (1971) and its northern extension was traced by Moriwaki (1975). Other two are subglacial valleys which are situated between St. Y8 and 9, and between S19 and 20. In the eastern part of the Lützow-Holm Bay, there are some deep submarine valleys but they are not parallel to the coast line (Omoto, 1976). Deep submarine and subglacial valleys to the east of the Syowa Station are arranged with interval of ca. 15 km, and such an arrangement may be originally controlled by local geological structures of bedrocks. Another deep subglacial depression observed between S58 and 66 may be a subglacial basin judging from it's scale. These submarine and subglacial valleys have been formed by glaciations.

The subglacial topography and longitudinal profiles of ice surface and bedrocks are fairly correlative with the coastal region near Mirnyy (Nudel'man, 1959), but different from the coastal region of Byrd (Robin *et al.*, 1970). Subglacial bedrock surface is situated nearly at mean sea level at the coast near Mirnyy Station with some deep subglacial valleys which reach below mean sea level, while it is situated far below mean sea level at the coast of Byrd Station.

The bedrock topography is smoother at the coastal region than inland (Figs. 8 and 9). From coastal region to inland, the bedrock surface increases altitude gradually and its range of undulation expands. Judging from the subaerial coastal geomorphology of Lützow-Holm Bay, the subglacial bedrock topography is considered as *roches moutonnée* between S80 and the shore, and especially giant *roches moutonnée* between S80 and 160. The above undulating low relief broken between S172 and 180 by the deepest subglacial valley in the Mizuho Plateau, i.e. Shirase Subglacial Trough (simply Shirase Trough) reaching 1800 m below mean sea level. Ishida (1970) reported that the trough between 70°S and 71°S might continue to Shirase Glacier and accord to the results obtained by U.S.S.R. traverse (Stroev *et al.* 1967). However the trough in his figures corresponds to the subglacial valleys observed by the present author between S130 and 170. Although the gravity data of Ishida's and the 10th party agree well with each other, it is difficult to find out such a deep subglacial valley from the gravity data. The Shirase Trough, if it existed, might join to the upstream of the Shirase Glacier and would continue to the upstream of Lambert Glacier to the east. Further southward from the Shirase Trough, the subglacial bedrock surface looks like *roches moutonnée* again. It is broken at S204 by the subglacial mountains which continue to S240 and A110 at least. The mountains are 1500 m a.s.l. in height and 1500 m in relative height which belong perhaps to the northern part of Vernadsky Mountains (Kapitza 1967). But such subglacial rises or mountains are impossible to distinguish from the gravity values.

Between Yamato and Vernadsky Mountains, the bedrock topography along 72°S is as undulated as giant *roches moutonnée*, which is a striking contrast to the bottom topography with complicated features of deep valleys and high mountains along 71°S. The subglacial deep valleys are located at the extension of the branches of Shirase Glacier and they surely continue to the upstream of the branches of Shirase Glacier. The complicated subglacial topography along 71°S resembles that between Sovetskaya Station and Gamburtsev Mountains (Robin *et al.*, 1970).

The lowland between Yamato and Vernadsky Mountains is named by the author Mizuho Subglacial Basin (simply Mizuho Basin), whose basin floor is about 150 km wide from east to west, and covered with ice about 2000 m thick.

At the west of Yamato Mountains, the echo data agree very well with gravity data. The mountains about 200 m to 800 m above ice surface are conspicuously glaciated. The subglacial bedrocks were sounded to range between 300 m to 2000 m in depth and evidently deeply scooped. The profiles of glacier surface and bedrock along the outlet glacier beetween D and E massifs are of the same category with those of the outlet glacier at the Penny Ice Cap in Baffin Island (Weber *et al.* 1970). The rise midway of the glacier bottom may reflect the north-south trend of geological structure parallel to the mountains. Subglacial valleys in Fig. 23 are shown separated between nunataks and the western extension of massifs, resemble to subglacial valleys revealed by Drewry (1972). The radio echo-sounding revealed the direction of ice movement scooping strongly bedrocks and the longitudinal profile of outlet glaciers at the west of Yamato Mountains.

5 Conclusion

The subglacial topography of Mizuho Plateau and around Yamato Mountains is summarized as following conclusions.

(1) Subglacial bedrock surface is nearly at mean sea level at the coastal region, east of the Syowa Station except two deep glaciated troughs between St. Y8 and 9, and between S19 and 20, and a subglacial basin between S58 and 66. The feature and origin of troughs are the same as the deep submarine valley in the Ongul Strait over 600 m below mean sea level. The ice surface and the bedrock surface are shown in Figs. 1, 6, 7, 8 and 9.

(2) Subglacial bedrock surface is gradually ascending to 500 m a.s.l. along the meridian of 43°E. Undulating bedrock surface (Fig. 10) seems to be giant *roches moutonnée* as observed at the coast of the Lützow-Holm Bay.

(3) The deepest subglacial valley sounded by the 14th party between S172 and 180 in the Mizuho Plateau, is 1800 m below mean sea level in depth, nearly 2000 m in relative depth (Fig. 10) and named Shirase Subglacial Trough (simply Shirase Trough) by the author. It may join to the upstream of the Shirase Glacier and continue to the upstream of the Lambert Glacier to the east. This deep valley divides the Enderby Land from East Antarctica proper.

(4) From S204, subglacial bedrock surface becomes complicated southward, and mountain and valley features appear. The mountains rise up to 1500 m a.s.l. and continue to S240 and A110. They perhaps belong to the northern part of Vernadsky Mountains crossing the East Antarctica.

(5) Contrasting subglacial topography along the routes of 71°S and 72°S are shown in Figures 11 and 12. Undulating low relief along 72°S is probably giant *roches moutonnée* and complicated features along 71°S are alternating valleys and mountains. Such a subglacial relief is reflected to ice surface. The subglacial valleys join the upstream of Shirase Glacier scooping out the bedrock surface.

(6) Between Yamato and Vernadsky Mountains, a broad and low undulating surface named Mizuho Subglacial Basin (Mizuho Basin) extends 150 km from east to west, which is covered with ice 2000 m in thickness (Fig. 11). The Mizuho Basin forests the southern half of Shirase Glacier.

(7) At the west of Yamato Mountains, the bottom topograply of the outlet glaciers was sounded between 300 m to 2000 m deep, and the glaciers scoop deeply bedrocks (Fig. 23).

(8) The gravity data ("go" values) correspond in general with the echo data except the case of high relief. The gravity data never present high relief such as detected at Shirase Trough or the Vernadsky Mountains, if not considered Bouguer anomaly.

(9) The geological structure south of Prince Harald and Prince Olav Coasts is inferred from the radio echo-sounding, the geological survey both on Yamato Mountains and ice-free area of Lützow-Holm Bay. Although the northwestern extension of Vernadsky Mountains has not been confirmed yet, the rises of bedrock surface or the trend of geological structure is probably continuous through Belgica Mountains, via Yamato Mountains, Botnnunten, to the ice-free Soya Coast. The subglacial rise is scooped at dominant glaciers such as Shirase Glacier deeply.

The author wishes to thank Professor Kou Kusunoki, National Institute of Polar Research and all the members of the JARE-10, especially members of the inland traverse party for their encouragement and cooperation, and Mr. Koutaro Yokoyama in charge of the radio echo-sounding of the 14th party.

The author appreciates Professor Kasuke Nishimura of Tohoku University who kindly encouraged the author to arrange and discuss on this study, and read this manuscript critically and gave useful suggestions.

Another thank is given to Professor Torao Yoshikawa at University of Tokyo who gave the author the chance to study glacial geomorphology.

The author would like to dedicate this paper to the late mother, who kindly encouraged and educated him.

References (*in Japanese)

Ageta, Y. (1971): Some aspects of the weather condition in the vicinity of the Mizuho Plateau, East Antarctica.* *Ant. Rec.* **41** 42–61

——— (1972): Some aspects of ablation of sastrugi and drifts in the area subjected to katabatic wind in Antarctica.* *ibid.* **43** 8–19

Ando, H. (1971): Preliminary report of the oversnow traverse of the 10th Japanese Antarctic Research Expedition in 1969–1970*. *ibid.* **39** 39–45

Bardin, V.I. and I.A. Suyetova (1967): Basic Morphometric Characteristics for Antarctica and Burget of the Antarctic Ice Cover. *JARE Sci. Rep., Special Issue* **1**, 92–100

Clough, J.W. and C.R. Bentley (1970): Measurements of electromagnetic wave velocity in the East Antarctic ice sheet. *I.S.A.G.E. Publ.* **86** Sec. 5, 115–128

Drewry, D.J. (1972): The contribution of radio echo-sounding to the investigation of Cenozoic tectonics and glaciation in Antarctica (in Polar Geomorphology. Compiled by R.J. Price and D.E. Sugdew) *Inst. Brit. Geogr. Special Publ.* **4**, 43–57.

Evans, S. (1963): Radio techniques for the measurement of ice thickness. *Polar Rec.* **11** 406–410

Fujiwara, K. (1964): Preliminary Report on the Morphology of the Inland Ice Sheet of the Mizuho Plateau, East Antarctica. *Ant. Rec.* **23** 1835–1845

——— (1971): Outline of Scientific Program and Its Results. (Rep. Jap. Trav. Syowa-South Pole., Polar Res. Cent. Natl. Sci. Mus.), *JARE Sci. Rep. Special Issue* **2**, 23–29

Fujiwara, K., Kakinuma, S., and Y. Yoshida (1971): Survey and Some Considerations on the Antarctic Ice Sheet. *ibid.* 30–48

——— **and Y. Endo** (1971): Preliminary Report of Glaciological Studies. *ibid.* 68–109

——— (1971): Soundings and Submarine Topography of the Glaciated Continental Shelf in Lützow-Holm Bay, East Antarctica*. *Ant. Rec.* **41** 81–103

Ishida, T. (1970): Glaciological research on the inland traverse of the 8th Japanese Antarctic Research Expedition. *I.S.A.G.E. Publ.* **86** 130–138

Kapitza, A.P. (1967): Antarctic Glacial and Subglacial Topography. *JARE Sci. Rep. Special Issue* **1** 82–91

Kikkawa, M. (1972): Medical Investigations on the Wintering Members of the 10th Japanese Antarctic Research Expedition 1. Circulatory Condition of Finger Tip in Antarctica. *Ant. Rec.* **43** 31–40

Kizaki, K. (1965): Geology and Petrography of the Yamato Sanmyaku, East Antarctica. *JARE Sci. Rep., Ser.* C, **3**

Kusunoki, K. (1971): General report of the wintering party of the 10th Japanese Antarctic Research Expedition 1968–1970. *Ant. Rec.* **40** 1–21

Meinardus, W. (1926): Die hypsographischen Kurven Grönlands und der Antarktis und die Normalform der Inlandeisoberfläche. *Petermanns Geogr. Mitt.* **72**

Moriwaki, K. (1975): Submarine Topography near Syowa Station, Antarctica*. *Ant. Rec.* **54** 101–115

Naruse, R., and K. Yokoyama (1975): Position, elevation and ice thickess of stations. (Glaciological Research Program in Mizuho Plateau-West Enderby Land, East Antarctica Part 3, 1973–1974). *JARE Data Rep.* **28** 7–47

Nudel'man, A.V. (1959): *Soviet Expeditions to the Antarctic, 1955–1959.* Moskva, Izd-vo. Akad. nauk USSR, 132p.

Omoto, K. (1970): Radio Echo Sounding of Antarctic Ice by JARE-10.* *Ann. Tohoku Geogr. Assoc.* **22** 162

——— (1976): Glacio-geomorphic Study on Submarine Morphology East of Lützow-Holm Bay, Antarctica. *Mem. Natl. Inst. Polar Res.*, Ser. C (in preparation).

Robin, G.de.Q., C.W.M. Swithinbank and B.M.E. Smith (1970): Radio echo exploration of the Antarctic ice sheet. *I.S.A.G.E. Publ.* **86** 97–115

Shimizu, H., R. Naruse, K. Omoto, and A. Yoshimura (1972): Position of Stations, Surface Elevation and Thickness of the Ice Sheet, and Snow Temperature at 10 m Depth in the Mizuho Plateau-West Enderby Land Area, East Antarctica, 1969–1971 (Glaciological Research Program in Mizuho Plateau-West Enderby Land Part 1, 1969–1971). *JARE Data Rep.* **17** 12–37

Stroev, P.A., Ushakov, S.A. and Frolov, A.I. (1967): Crustal structure in the marginal zone of Antarctica. Gravimetry. 6. Results of researches on international geophysical projects. *Academy of sciences of the U.S.S.R. Soviet geophysical committee.*

Weber, J.R. and P. Andrieux (1970): Rader Sounding on the Penny Ice Cap, Baffin Island. *Jour. Glac,* **9** (55), 49–54

Yoshida, Y. (1961): Preliminary Report on Geomorphological Survey of the Yamato Mountains, East Antarctica. *Ant. Rep.* **13** 1077–1080

——— **and K. Fujiwara** (1963): Geomorphology of the Yamato (Queen Fabiola) Mountains*. *ibid.* **18** 1519–1544

Yoshida, M., and H. Ando (1971): Geological survey in the vicinity of Lützow-Holm Bay and the Yamato Mountains, East Antarctica. *ibid.* **39** 46–54

———, **Y. Ageta, and M. Yagi** (1971): Newly found inland moraine fields near Syowa Station in 1970. *ibid.* **39** 55–61

———, **H. Ando, K. Omoto, R. Naruse and Y. Ageta** (1971): Discovery of meteorites near Yamato Mountains, East Antarctica. *ibid.* **39** 62–65

——— **and A. Yoshimura** (1972): Gravimetric Survey in the Mizuho Plateau West Enderby Land Area, East Antarctica, 1969–1971 (Glaciological Research Program in Mizuho Plateau-West Enderby Land Part 1, 1969–1971). *JARE Data Rep.* **17** 168–217

Yoshino, T. and T. Eto (1971): Radio Echo Sounding of Antarctic Ice (Report of the Japanese Traverse Syowa-South Pole 1968–1969, Edited by M. Murayama). *JARE Sci. Rep. Special Issue* **2** 125–130

Table 3. Geodetic positions of the station, surface elevation of ice sheet, ice thickness, bedrock elevation, and gravity value reduced to sea level by free air reduction, along the inland traverse route of JARE-10

Station				Radio Echo Sounding			gravity value
No.	Latitude	Longitude	Elevation (m)	One-way echo time (μs)	Ice thickness (m)	Bedrock elevation (m)	go (mgal)
							982
S 16	□69°01′57″S	□40°02′50″E	553	2.75	470	83	576.7
17	69 01.9′	40 04	583	2.93	501	82	577.8
18	69 01.7	40 07	609	4.40*	752	−143	571.2
19	69 01.5	40 10	634	6.60	1129	−495	548.0
20	69 01.5	40 12	653	7.30*	1248	−595	551.7
21	69 01.6	40 15	699	3.42	585	114	566.1
22	69 01.7	40 18	743	4.78	817	− 74	568.3
23	69 01.8	40 21	771	4.59	785	− 14	570.4
24	69 01.9	40 24	811	4.18	715	96	573.5
25	69 02.2	40 27	844	4.23	723	121	572.2
26	69 02.3	40 29	870	5.00*	855	15	572.7
27	69 02.5	40 32	893	6.00*	1026	−133	570.6
28	69 02.7	40 35	916	5.67	970	− 54	570.7
29	69 02.8	40 38	935	5.70*	975	− 40	572.1
30	69 03.1	40 40	961	5.43	929	32	570.8
31	○69 03.3	○40 43	981	5.65	966	15	568.0
32	69 03.6	40 46	994	6.63	1134	−140	566.5
33	69 03.9	40 48	1014	6.55*	1120	−106	567.8
34	69 04.2	40 51	1030	6.07	1038	− 8	566.9
35	69 04.4	40 54	1046	6.48	1108	− 62	568.4
36	69 04.8	40 56	1064	6.25	1069	− 5	571.0
37	69 04.8	40 59	1074	6.80*	1163	− 89	571.2
38	69 04.9	41 02	1088	6.43	1100	− 12	568.9
39	69 04.8	41 05	1099	7.00	1197	− 98	565.5
40	69 04.7	41 07	1112	6.43	1100	12	566.8
41	69 04.6	41 10	1124	6.38	1091	33	567.9
42	69 04.6	41 13	1138	6.63	1134	4	569.4
43	69 04.5	41 15	1148	6.55	1120	28	569.6
44	69 04.3	41 18	1164	7.18	1228	− 64	571.5
45	69 04.4	41 21	1179	6.95	1189	− 10	571.1
46	69 04.5	41 24	1188	6.93	1185	3	568.5
47	69 04.3	41 26	1184	7.22	1235	− 51	565.4
48	69 04.2	41 29	1200	7.25	1240	− 40	564.8
49	69 04.2	41 32	1208	7.05*	1206	2	567.2
50	69 04.2	41 35	1215	7.05	1206	9	568.7
51	69 04.1	41 37	1217	7.55*	1291	− 74	568.8
52	69 04.1	41 40	1227	7.07	1209	18	568.7
53	69 04.0	41 43	1233	6.98	1194	39	570.7
54	69 04.1	41 46	1259	7.25*	1240	19	573.6
55	69 04.2	41 48	1271	7.30*	1248	23	572.4
56	69 03.7	41 51	1274	7.38*	1262	12	571.5
57	69 03.8	41 54	1276	7.10*	1214	62	571.7
58	69 04.2	41 57	1287	7.30*	1248	39	574.2
59	69 04.4	41 59	1307	7.70*	1317	− 10	571.3
60	69 04.6	42 02	1332	7.79	1332	0	563.0
61	69 05.0	42 04	1335	8.70*	1488	−153	557.7

Table 3. (Continued)

Station				Radio Echo Sounding			gravity value
No.	Latitude	Longitude	Elevation (m)	One-way echo time (μs)	Ice thickness (m)	Bedrock elevation (m)	go (mgal)
							982
62	69°05.'2'S	42°07'E	1341	8.66	1481	−140	554.9
63	69 05.3	42 09	1348	8.40	1436	− 88	553.4
64	69 05.5	42 12	1356	8.60*	1471	−115	553.4
65	69 05.8	42 15	1362	8.75*	1496	−134	555.1
66	69 05.9	42 18	1366	7.85*	1342	24	557.7
67	69 06.0	42 21	1363	7.20*	1231	132	558.5
68	69 06.2	42 23	1380	7.52	1286	94	557.2
69	69 06.4	42 26	1381	8.05*	1377	4	555.1
70	○ 69 06.9	○ 42 29	1388	8.35	1428	− 40	552.4
71	69 07.9	42 29	1403	8.13	1390	13	555.7
72	69 09.0	42 30	1409	8.28*	1416	− 7	558.6
73	69 10.0	42 30	1419	8.25	1411	8	560.3
74	69 11.0	42 31	1422	8.25	1411	11	561.6
75	69 12.1	42 32	1435	8.35	1428	7	563.5
76	69 13.1	42 32	1444	8.05	1377	67	564.4
77	69 14.2	42 33	1451	8.65	1479	− 28	563.6
78	69 15.2	42 34	1459	8.45	1445	14	565.9
79	69 16.2	42 34	1468	8.40	1436	32	567.4
80	69 17.3	42 35	1473	8.90	1522	− 49	569.3
81	69 18.4	42 36	1476	7.90	1351	125	573.5
82	69 19.4	42 36	1489	8.50*	1454	35	576.9
83	69 20.5	42 37	1499	8.15	1394	105	577.8
84	69 21.5	42 38	1518	7.80	1334	184	574.3
85	69 22.5	42 38	1522	—	—		572.3
86	69 23.5	42 39	1526	—	—		575.6
87	69 24.6	42 40	1534	—	—		580.6
88	69 25.6	42 41	1543	—	—		584.5
89	69 26.7	42 41	1551	—	—		585.9
90	69 27.7	42 42	1560	8.40	1436	124	588.6
91	69 28.8	42 43	1569	—	—		587.0
92	69 29.8	42 43	1568	—	—		587.2
93	69 30.9	42 44	1570	—	—		596.3
94	69 31.9	42 45	1579	8.54	1460	119	604.8
95	69 32.8	42 46	1588	8.40	1436	152	611.2
96	69 33.9	42 47	1594	8.10	1385	209	617.2
97	69 34.9	42 48	1605	8.08	1382	223	622.2
98	69 36.0	42 48	1614	7.58	1296	318	623.1
99	69 37.0	42 49	1618	—	—		617.6
100	69 38.1	42 50	1630	8.00	1368	262	613.8
101	69 39.1	42 50	1631	—	—		613.3
102	69 40.1	42 51	1636	—	—		615.4
103	69 41.1	42 52	1643	—	—		616.8
104	69 42.2	42 52	1651	—	—		622.2
105	69 43.2	42 53	1656	—	—		626.6
106	69 44.3	42 54	1660	7.63	1305	355	634.0
107	69 45.4	42 55	1673	7.75	1325	348	635.3
108	69 46.4	42 55	1684	8.70	1488	196	629.3
109	69 47.5	42 56	1690				631.6

Table 3. (Continued)

Station				Radio Echo Sounding			gravity value
No.	Latitude	Longitude	Elevation (m)	One-way echo time (μs)	Ice thickness (m)	Bedrock elevation (m)	go (mgal)
							982
S 110	69°48.5′S	42°56′E	1696	7.16	1224	472	647.0
111	69 49.5	42 57	1724	6.45	1103	621	658.3
112	69 50.6	42 58	1736	7.51	1284	452	658.5
113	69 51.7	42 59	1747	7.80	1334	413	657.5
114	69 52.7	43 00	1754	7.63	1305	449	658.7
115	69 53.8	43 01	1758	6.40	1094	664	665.7
116	69 54.8	43 02	1763	6.73	1151	612	670.0
117	69 55.9	43 03	1774	7.05*	1206	568	669.2
118	69 56.9	43 03	1816	7.40	1265	551	672.2
119	69 58.0	43 04	1833	8.70*	1488	345	666.7
120	69 59.0	43 04	1845	9.25*	1582	263	659.3
121	70 00.1	43 05	1850	8.95	1531	319	660.8
122	○ 70 01.1	○ 43 06.5	1853	9.04	1546	307	664.1
123	70 02.1	43 06	1859	8.05	1377	482	668.2
124	70 03.2	43 06	1865	7.10	1214	651	674.6
125	70 04.2	43 07	1876	7.30	1248	628	676.6
126	70 05.2	43 07	1883	8.30	1419	464	675.8
127	70 06.3	43 06	1886	7.58	1296	590	675.6
128	70 07.3	43 06	1887	8.30	1419	468	668.9
129	70 08.4	43 06	1900	—	—		656.9
130	70 09.5	43 06	1900	—	—		656.2
131	70 10.4	43 06	1907	9.05	1548	359	660.2
132	70 11.5	43 06	1924	9.10	1556	368	656.9
133	70 12.5	43 06	1923	—	—		651.6
134	70 13.5	43 06	1917	—	—		651.3
135	70 14.6	43 06	1909	—	—		654.3
136	70 15.6	43 06	1914	—	—		656.4
137	70 16.7	43 06	1923	—	—		655.7
138	70 17.7	43 06	1924	—	—		652.9
139	70 18.7	43 06	1925	—	—		650.6
140	70 19.8	43 06	1934	—	—		646.7
141	70 20.9	43 06	1944	—	—		644.9
142	70 21.9	43 06	1945	11.00	1881	64	644.2
143	70 22.9	43 06	1946	—	—		641.5
144	70 24.0	43 06	1946	—	—		670.7
145	70 25.0	43 06	1944	—	—		636.9
146	70 26.1	43 06	1950	—	—		633.3
147	70 27.1	43 06	1954	—	—		628.2
148	70 28.1	43 06	1952	—	—		631.5
149	70 29.2	43 06	1953	—	—		640.6
150	70 30.0	43 04	1971	7.70	1317	654	645.0
151	○ 70 31.0	○ 43 05	1975	—	—		644.1
152	70 31.9	43 06	1978	—	—		645.2
153	70 32.9	43 05	1979	—	—		646.6
154	70 34.0	43 05	1986	—	—		647.1
155	70 35.0	43 05	1992	—	—		648.7
156	70 36.1	43 06	1997	—	—		650.7
157	70 37.1	43 06	2002	10.85	1855	147	650.5

Table 3. (Continued)

Station				Radio Echo Sounding			gravity value
No.	Latitude	Longitude	Elevation (m)	One-way echo time (μs)	Ice thickness (m)	Bedrock elevation (m)	go (mgal)
							982
S 158	70°39′2 S	43°06′ E	2005	11.00	1881	124	645.1
159	70 39.2	43 06	2006	—	—		640.4
160	70 40.2	43 06	2008	8.30	1419	589	636.7
161	70 41.2	43 06	2012	—	—		640.0
162	70 42.3	43 06	2020	—	—		649.0
163	70 43.3	43 07	2025	—	—		654.4
164	70 44.3	43 07	2034	—	—		657.9
165	70 45.3	43 07	2035	12.55	2146	−111	659.2
166	70 46.4	43 07	2027	12.50	2138	−111	659.6
167	70 47.4	43 07	2027	12.50	2138	−111	661.6
168	70 48.4	43 07	2026	—	—		661.7
169	70 49.4	43 07	2035	13.50	2309	−274	662.0
170	• 70 50′38″	• 43 11′32″	2034	11.50	1967	67	669.8
171	70 51.1	43 05	2026	13.11	2241	−215	674.4
172	70 51.6	43 02	2040	11.13	1903	137	678.9
173	70 52.2	43 00	2034	11.13	1903	131	682.5
174	70 52.8	42 57	2018	△14.68*	2511	− 493	680.5
175	70 53.8	42 56	2036	△22.11*	3780	−1744	683.5
176	70 54.8	42 56	2063	△22.63*	3870	−1807	683.4
177	70 55.8	42 56	2064	△18.95*	3240	−1176	682.9
178	70 56.8	42 56	2061	△17.63*	3015	− 954	688.1
179	70 57.9	42 56	2062	△11.84*	2025	37	693.1
180	70 58.9	42 57	2075	△11.68*	1998	77	698.5
181	70 59.9	42 57	2085	△11.37*	1944	141	702.8
182	71 00.9	42 57	2100	△10.53*	1800	300	704.7
183	71 01.9	42 57	2133	△11.16*	1908	225	702.7
184	71 03.0	42 57	2139	△12.32	2106	33	697.1
185	71 04.0	42 57	2114	11.13	1903	211	697.2
186	71 05.0	42 58	2150	△11.63*	1989	161	700.6
187	71 06.0	42 58	2158	—	—		700.9
188	71 07.0	42 58	2159	—	—		704.8
189	71 08.1	42 58	2173	△12.16*	2079	94	708.4
190	71 09.1	42 58	2180	11.63	1989	191	709.9
191	71 10.1	42 58	2183	11.75	2009	174	709.8
192	71 11.2	42 58	2195	△12.16	2079	116	709.5
193	71 12.2	42 59	2207	△12.21	2088	119	710.4
194	71 13.2	42 59	2211	△12.42*	2124	87	710.3
195	71 14.2	42 59	2208	△12.37*	2115	93	711.8
196	71 15.3	42 59	2217	△17.68*	1998	219	714.1
197	71 16.3	43 00	2240	△12.00*	2052	188	714.0
198	71 17.3	43 00	2251	△12.21	2088	163	712.3
199	71 18.3	43 00	2257	△12.63	2160	97	710.2
200	71 19.4	43 00	2261	△13.95	2385	−124	708.2
201	71 20.4	43 00	2260	△13.63*	2331	− 71	708.3
202	71 21.4	43 00	2261	△12.68*	2169	92	711.6
203	71 22.4	43 01	2274	△12.63*	2160	114	713.9
204	71 23.5	43 01	2294	△ 9.26*	1584	710	715.4
205	71 24.5	43 01	2303	△ 8.63*	1476	827	715.0

Table 3. (Continued)

Station				Radio Echo Sounding			gravity value
No.	Latitude	Longitude	Elevation (m)	One-way echo time (μs)	Ice thickness (m)	Bedrock elevation (m)	go (mgal)
							982
S 206	71°25.5′S	43°01′E	2310	△14.16*	2421	−111	713.7
207	71 26.5	43 02	2312	—	—		712.3
208	71 27.5	43 02	2315	—	—		715.4
209	71 28.5	43 02	2317	△13.42*	2295	22	718.1
210	71 29.6	43 03	2332	△ 6.26	1071	1261	721.5
211	71 30.6	43 03	2342	△13.32*	2277	65	723.1
212	71 31.6	43 03	2346	—	—		725.0
213	71 32.6	43 03	2356	△ 6.53	1116	1240	726.5
214	71 33.7	43 03	2369	△ 6.53*	1116	1253	727.0
215	71 34.7	43 04	2374	△14.21*	2430	−56	727.2
216	71 35.7	43 04	2377	△13.68*	2340	37	728.8
217	71 36.7	43 04	2388	△12.37*	2115	273	730.3
218	71 37.7	43 04	2401	△13.79*	2358	43	732.1
219	71 38.7	43 04	2403	△ 8.68*	1485	918	732.9
220	71 39.7	43 04	2410	△ 6.84*	1170	1240	737.6
221	71 40.8	43 05	2422	△13.11*	2241	181	739.9
222	71 41.8	43 05	2433	△13.21*	2259	174	740.7
223	71 42.8	43 05	2443	△ 8.37*	1431	1012	741.6
224	71 43.8	43 05	2453	△13.63*	2331	122	743.1
225	71 44.8	43 05	2462	△14.21*	2430	32	743.8
226	71 45.8	43 06	2468	△ 7.84*	1341	1127	746.8
227	71 46.8	43 06	2473	△ 8.11*	1386	1087	749.6
228	71 47.8	43 06	2485	△ 8.95*	1530	955	752.4
229	71 48.9	43 06	2494	△ 6.74*	1152	1342	753.2
230	71 49.9	43 06	2506	△ 8.00*	1368	1138	753.8
231	71 50.9	43 07	2511	△13.95*	2385	126	754.6
232	71 51.9	43 07	2515	△ 7.84*	1341	1174	756.9
233	71 53.0	43 07	2522	△ 5.84*	999	1523	759.3
234	71 54.0	43 08	2528	△ 8.95	1530	998	763.0
235	71 55.0	43 08	2534	△12.21	2088	446	765.8
236	71 56.0	43 08	2550	—	—		769.1
237	71 57.0	43 08	2567	△13.58*	2322	245	769.2
238	71 58.1	43 08	2574	△ 5.68*	972	1602	769.3
239	71 59.1	43 08	2580	△ 6.84*	1170	1410	770.6
240	(●) 72°00′08″	(●) 43°09′51″	2591	—	—		770.5
A 163	72°01.5′ S	43°08.0′ E	2604				776.0
162	72 00.2	43 07	2585	△ 8.68*	1485	1115	775.1
161	72 01.5	43 04	2599				781.0
160	72 00.2	43 04	2565	△13.74*	2349	232	
159	72 01.5	43 01	2586				783.7
158	71 59.8	42 58	2540	11.25	1924	616	
157	72 01.5	42 55	2568				782.5
156	72 00.1	42 53	2544	—	—		
155	72 01.4	42 50	2573				779.2
154	72 00.8	42 47	2561				773.0
153	71 59.1	42 48	2533	7.55	1291	1242	771.0
152							

Table 3. (Continued)

Station				Radio Echo Sounding			gravity value
No.	Latitude	Longitude	Elevation (m)	One-way echo time (μs)	Ice thickness (m)	Bedrock elevation (m)	go (mgal)
							982
A 151	71°58.5′ S	42°44′ E	2535	△ 6.84*	1170	1381	
150	71 59.5	42 41	2549				766.9
149	71 58.5	42 40	2542	△ 9.79*	1674	882	
148							
147	71 58.1	42 37	2536	△ 7.42*	1269	1281	769.4
146	71 58.9	42 34	2545				773.4
145	71 58.0	42 34	2527	△ 12.11*	2070	471	
144	71 58.9	42 29	2536				779.7
143	71 57.8	42 24	2491	△ 12.58*	2151	357	776.4
142	71 59.3	42 26	2534				781.7
141	71 58.5	42 18	2500	△ 6.16*	1053	1463	
140	71 59.9	42 21	2520				782.2
139	71 59.3	42 16	2503	—	—		
138	72 00.5	42 15	2499				780.2
137	71 59.7	42 13	2509	—	—		
136	72 00.3	42 13	2509				776.7
135	71 59.8	42 11	2509	△ 12.74*	2178	346	772.0
134	72 00.5	42 08	2510				774.2
133	71 59.5	42 06	2514	△ 13.16*	2250	279	
132	72 00.8	42 03	2518				773.5
131	72 00.0	42 00	2530	△ 7.00*	1197	1337	
130	72 00.9	41 56	2527				773.7
129	71 59.9	41 53	2521	△ 12.47*	2133	402	
128	72 00.9	41 50	2533				777.0
127	72 00.0	41 47	2535	△ 14.37*	2457	82	786.1
126	72 01.1	41 47	2545				783.3
125	71 59.9	41 43	2533	△ 12.21*	2088	448	
124	72 01.4	41 40	2533				791.5
123	72 00.5	41 39	2529	△ 11.05*	1890	643	
122	72 01.6	41 36	2544				
121	72 00.1	41 36	2530	△ 12.89*	2205	328	790.9
120	72 01.5	41 33	2537				
119	72 00.1	41 31	2504	—	—		790.2
118	72 01.0	41 26	2528				
117	72 00.0	41 27	2511	△ 12.05*	2061	454	786.2
116	72 00.8	41 23	2521				786.5
115	72 00.0	41 24	2507	△ 12.16*	2079	431	785.6
114	72 00.4	41 21	2511				
113	71 59.5	41 18	2498	△ 7.63*	1305	1196	783.0
112	71 59.9	41 15	2504				
111	71 59.4	41 15	2499	△ 7.00*	1197	1305	776.3
110	71 59.9	41 12	2499				
109	71 58.7	41 10	2485	△ 12.05*	2061	428	777.5
108	71 59.7	41 08	2492				
107	71 58.7	41 04	2481	△ 12.16*	2079	406	779.2
106	71 59.4	41 01	2483				777.4
105	71 58.3	40 58	2479	△ 13.79*	2358	124	772.2
104	71 59.3	40 54	2482				

Table 3. (Continued)

Station				Radio Echo Sounding			gravity value
No.	Latitude	Longitude	Elevation (m)	One-way echo time (μs)	Ice thickness (m)	Bedrock elevation (m)	go (mgal)
							982
A103	71°58.4′ S	40°52′ E	2473	△ 12.63*	2160	316	
102	71 59.3	40 49	2477				772.3
101	71 58.2	40 44	2469	△ 12.63*	2160	312	
100	71 59.3	40 43	2479				773.2
099	71 57.9	40 38	2463	△ 13.58*	2322	144	776.0
098	71 59.2	40 35	2475				776.2
097	71 57.0	40 31	2453	△ 11.32*	1935	522	
096	71 58.5	40 27	2462				778.9
095	71 57.0	40 26	2453	△ 12.11*	2070	382	
094	71 58.2	40 20	2457				787.7
093	71 56.4	40 15	2417	—	—		782.4
092	71 58.3	40 16	2460				791.5
091	71 56.8	40 10	2426	—	—		
090	71 58.3	40 08	2446				783.1
089	71 56.7	40 03	2427	△ 12.58	2151	275	775.5
088							
087	71 56.7	39 57	2436	△ 12.68*	2169	269	778.1
086	71 58.2	39 54	2450				779.5
085	71 57.0	39 52	2444	△ 12.11	2070	372	
084	71 58.0	39 48	2448				780.4
083	71 56.0	39 46	2430	△ 12.37*	2115	314	
082	71 57.5	39 41	2445				781.2
081	71 55.6	39 36	2420	△ 12.53*	2142	277	
080	71 57.1	39 37	2440				778.5
079	71 55.6	39 31	2424	△ 12.37*	2115	307	
078	71 56.9	39 32	2433				775.4
077	71 55.5	39 28	2418	△ 12.26*	2097	320	
076	71 56.8	39 28	2426				775.3
075	(•) 71°55′21″	(•) 39°23′45″	2412	△ 12.63*	2160	251	772.0
074	71 56.4	39 21	2421				774.4
073	71 55.2	39 18	2414	△ 12.74*	2178	235	
072	71 56.4	39 17	2430				776.1
071	71 55.4	39 15	2417	△ 11.21*	1917	499	
070	71 56.4	39 13	2431				779.7
069	71 54.5	39 10	2406	△ 11.63*	1989	416	
068	71 55.6	39 06	2422				784.4
067	71 54.8	39 02	2404	△ 11.58*	1980	421	
066	71 55.6	39 01	2423				789.9
065	71 54.3	38 57	2384	△ 10.05*	1719	663	791.7
064	71 55.6	38 52	2408				795.3
063	71 54.0	38 51	2387	—	—		
062	71 55.4	38 47	2406				795.5
061	71 54.0	38 43	2397	△ 10.53*	1800	597	
060	71 54.9	38 39	2404				786.7
059	71 53.7	38 35	2392	△ 10.21*	1746	646	
058	71 55.3	38 30	2408				785.6
057	71 54.0	38 29	2399	△ 9.95*	1701	697	785.8
056	71 55.5	38 24	2413				784.1

Table 3. (Continued)

Station				Radio Echo Sounding			gravity value
No.	Latitude	Longitude	Elevation (m)	One-way echo time (μs)	Ice thickness (m)	Bedrock elevation (m)	go (mgal)
							982
A 055	71°54.5′S	38°19′E	2405	△ 11.32*	1935	469	
054	71 55.7	38 20	2416				786.4
053	71 54.7	38 14	2409	△ 12.00*	2052	358	
052	71 55.9	38 12	2425				793.4
051	71 54.5	38 08	2414	9.75	1667	747	
050	71 55.5	38 02	2422				791.3
049	71 54.2	37 59	2412	9.63	1647	765	798.3
048							
047	71 54.0	37 52	2409	9.84	1683	726	
046	71 54.6	37 49	2408				791.7
045	71 53.4	37 46	2398	△ 10.58	1809	590	
044	71 54.7	37 41	2411				788.0
043	71 53.6	37 36	2404	△ 9.47*	1620	785	
042	71 54.8	37 34	2413				786.2
041	71 53.6	37 29	2411	9.25	1582	829	
040	71 55.0	37 24.3	2425				788.6
039	71 53.6	37 20	2419	—	—		790.6
038	71 54.6	37 15	2430				789.5
037	71 53.6	37 14	2426	△ 10.53	1800	627	
036	71 53.8	37 12	2431				796.1
035	71 53.2	37 12	2421	8.00	1368	1053	
034	71 53.3	37 10	2422				802.2
033	71 52.4	37 10	2409	7.28*	1245	1164	
032	71 53.1	37 05	2414				797.3
031	71 51.6	37 03	2410	9.57	1637	773	794.5
030	71 52.8	36 59.9	2414				790.7
029	71 51.1	36 57	2395	△ 9.89*	1692	702	
028	71 52.2	36 55	2397				798.4
027	71 50.5	36 51	2376	8.05	1377	999	
026	71 56.8	36 50	2395				805.2
025	71 50.5	36 48	2377	8.20	1402	975	796.7
024							
023	71 50.3	36 44	2382	8.05	1377	1005	
022	71 50.1	36 39	2375				
021	71 51.3	36 39	2392	8.18	1399	976	791.8
020	71 50.9	36 36	2388				797.9
019	71 51.9	36 34	2387	8.65	1479	909	801.4
018	71 50.8	36 31	2377				
017	71 52.6	36 27	2376	6.40*	1094	1283	827.1
016	71 50.8	36 27	2370				
015	71 51.7	36 23	2353	5.40	923	1447	822.9
014	71 50.6	36 22	2351	3.45*	590	1761	829.8
013	71 50.4	36 18	2336				825.0
012	71 50.4	36 22	2351				832.9
011	71 49.43	36 22.31	2334	△ 7.79*	1332	1002	
010	71 50.0	36 20	2338	2.28	390	1948	842.8
009	71 48.9	36 20	2296				841.5
008	71 48.8	36 16	2286	3.25	556	1730	

Table 3. (Continued)

Station				Radio Echo Sounding			gravity value
No.	Latitude	Longitude	Elevation (m)	One-way echo time (μs)	Ice thickness (m)	Bedrock elevation (m)	go (mgal)
							982
A007							
006	71°49.8′ S	36°17′ E	2318	7.05	1206	1112	
005							
004	71 48.6	36 13	2269	3.48*	595	1674	
003	71 48.0	36 11	2251	2.55	436	1815	838.5
002	71 47.2	36 11	2279				
001	• 71°47′28.1″	• 36°12′12.2″	2254				
B1	71°48′ S	36.2°E	2242	2.35*	402	1840	
2	71 48	36.2	2224	2.63	450	1774	
3	71 47	36.1	2217	6.10*	1043	1174	808.5
4	71 46	36.1	2202	5.20	889	1313	
5	71 46	36.1	2182	5.20*	889	1293	805.2
6	71 45	36.0	2170	4.20	718	1452	
7	71 45	36.0	2156	3.65	624	1532	
8	71 45	36.0	2144	3.63*	621	1523	
9	71 45	35.9	2143	1.90	325	1818	
10	71 44	35.9	2157	—	—		
11	71 44	35.8	2122	—	—		
12	71 44	35.8	1991	—	—		834.1
13	71 43	35.7	1933	2.95	505	1428	807.6
14	71 42	35.7	1918	4.60*	787	1131	794.6
15	71 41	35.6	1888	4.25*	727	1161	782.6
16	71 40	35.6	1877	7.13*	1219	658	771.4
17	71 39	35.5	1857	5.90*	1009	833	772.9
18	71 38	35.5	1847	6.12*	1047	800	774.4
19	71 37	35.5	1819	10.80*	1847	−28	773.8
20	71 36	35.5	1800	5.20*	889	911	777.1
21	71 35	35.5	1793	3.83*	655	1138	777.9
22	71 34	35.5	1765	6.00*	1026	739	769.5
23	71 33	35.5	1750	5.36*	917	833	766.3
24	71 32	35.5	1740	4.48	766	974	773.4
25	71 31	35.5	1724	2.65*	453	1271	785.5
26	71 30	35.4	1713	3.43	587	1126	765.8
27	71 30	35.4	1705	5.00*	855	850	755.4
28	71 29	35.4	1704	5.80	992	712	744.1
29	71 28	35.3	1705	—	—		733.5
30	71 28	35.3	1718	7.35*	1257	461	744.3
31	71 27	35.4	1700	—	—		753.0
32	71 26	35.3	1694	6.06	1036	658	743.8
33	71 25	35.3	1680	7.05*	1206	474	743.3
34	71 24	35.4	1663	5.70	975	688	742.4
35	71 24	35.4	1649	5.60*	958	691	739.4
36	71 23	35.4	1635	5.64	964	671	733.9
37	71 22	35.4	1632	8.10*	1385	247	726.9
38	71 21	35.4	1643	—	—		726.4
39	71 20	35.4	1638	—	—		727.1
40	71 19	35.3	1641	—	—		720.0

Table 3. (Continued)

Station				Radio Echo Sounding			gravity value
No.	Latitude	Longitude	Elevation (m)	One-way echo time (μs)	Ice thickness (m)	Bedrock elevation (m)	go (mgal)
							982
B41	71°20′ S	35.4° E	1630	5.00	855	775	729.5
42	71 21	35.4	1647	5.30*	906	741	728.1
43	71 20	35.5	1671	7.30	1248	423	722.3
44	71 20	35.5	1671	7.80*	1334	337	716.5
45	71 20	35.6	1685	8.60*	1471	214	718.5
46	71 21	35.6	1705	11.12*	1902	−197	722.7
47	71 22	35.7	1743	11.33*	1937	−194	724.8
48	71°23.1′	35°41.1′	1800	6.50*	1112	688	736.4
C1	71°23.6′S	35°44.6′E	1813	4.10*	701	1112	754.6
2	71 21.9	35 48.1	1831	3.68	629	1203	755.6
3	71 21.4	35 50.9	1848	6.40*	1094	754	749.0
4	71 20.8	35 53.7	1828	4.83*	826	1002	749.4
5	71 20.4	35 56.5	1808	4.70*	804	1004	739.8
6	71 19.7	35 59.3	1796	6.51	1113	683	717.9
7	71 19.3	36 02.1	1794	—	—		704.4
8	71 18.7	36 04.9	1790	△9.11*	1557	233	695.5
9	71 18.2	36 07.8	1779	△7.16*	1224	555	690.6
10	71 17.6	36 10.5	1768	6.85	1171	597	703.6
11	71 17.2	36 13.2	1764	8.15*	1394	370	712.8
12	71 16.5	36 16.0	1757	7.50*	1283	474	717.7
13	71 16.1	36 18.8	1754	7.35*	1257	497	724.6
14	71 15.5	36 21.6	1758	6.75	1154	604	725.5
15	71 15.0	36 24.4	1763	8.35*	1428	335	720.2
16	71 14.4	36 27.2	1759	7.50	1283	476	717.8
17	71 13.9	36 30.0	1759	7.25	1240	519	714.0
18	71 13.3	36 32.6	1768	8.00	1368	400	702.0
19	71 12.6	36 34.2	1762	8.10	1385	377	696.8
20	71 11.9	36 36.6	1764	10.00	1710	54	685.7
21	71 11.5	36 39.4	1766	5.44*	930	836	680.5
22	71 11.0	36 41.5	1756	7.80	1334	422	693.0
23	71 10.6	36 44.3	1759	6.85	1171	588	696.6
24	71 10.1	36 46.9	1771	△8.58	1467	304	685.5
25	71 09.7	36 49.5	1782	5.00	855	927	674.4
26	71 09.2	36 52.2	1779	6.00*	1026	753	670.3
27	71 08.8	36 55.6	1786	5.00*	855	931	671.4
28	71 08.2	36 58.4	1787	4.55*	778	1009	675.2
29	71 08.2	37 01.6	1787	4.70*	804	983	682.1
30	71 08.1	37 04.7	1792	4.80*	821	971	683.0
31	71 08.1	37 07.9	1798	5.60*	958	840	679.2
32	71 08.6	37 11.1	1798	5.00*	855	943	687.2
33	71 08.1	37 14.3	1799	△9.79	1674	125	696.9
34	71 08.0	37 17.5	1897	9.00	1539	258	706.2
35	71 08.0	37 20.7	1801	△8.74*	1494	307	714.3
36	71 08.0	37 23.9	1803	△8.37*	1431	372	716.7
37	• 71°07′53″	• 37°27.5′	1805	8.67*	1483	322	715.6
38	71 07.9	37 30.3	1806	8.50	1454	352	713.3
39	71 07.8	37 33.5	1808	8.50*	1454	354	715.7

Table 3. (Continued)

Station				Radio Echo Sounding			gravity value
No.	Latitude	Longitude	Elevation (m)	One-way echo time (μs)	Ice thickness (m)	Bedrock elevation (m)	go (mgal)
							982
C 40	71°07.8′S	37°36.6′E	1813	7.23	1245	568	719.6
41	71 07.7	37 39.8	1815	8.80*	1505	310	716.7
42	71 07.7	37 43.0	1811	8.80*	1505	306	713.9
43	71 07.6	37 46.2	1808	8.13*	1390	418	713.0
44	71 07.6	37 49.4	1807	6.50*	1112	695	719.8
45	71 07.5	37 52.5	1799	6.00	1026	773	720.2
46	71 07.5	37 55.7	1793	7.05*	1206	587	717.3
47	71 07.3	37 58.9	1799	8.00	1368	431	709.9
48	71 07.3	38 02.1	1793	9.67	1654	139	699.1
49	71 07.2	38 05.3	1792	5.05	864	928	692.9
50	71 07.2	38 08.4	1796	8.15	1394	402	690.7
51	71 07.1	38 11.6	1786	9.85	1684	102	685.9
52	71 07.1	38 14.8	1768	8.55	1462	306	682.8
53	71 07.0	38 18.0	1757	△ 9.95*	1701	56	676.0
54	71 07.0	38 21.2	1763	9.60	1642	121	673.1
55	71 06.9	38 24.3	1757	△ 9.95*	1701	56	670.6
56	71 06.9	38 27.5	1745	△ 10.00*	1710	35	666.7
57	71 06.8	38 30.7	1730	—	—		657.9
58	71 06.8	38 33.9	1725	△ 7.84*	1341	384	645.1
59	71 06.7	38 37.2	1721	△ 8.58*	1467	254	634.1
60	71 06.7	38 40.3	1729	△ 9.63*	1647	82	634.4
61	71 06.6	38 43.5	1744	△ 10.05*	1719	25	641.9
62	71 06.6	38 46.7	1749	—	—		648.1
63	71 06.5	38 49.8	1748	△ 12.26*	2097	−349	653.6
64	71 06.5	38 53.0	1741	△ 11.11	1899	158	658.5
65	71 06.4	38 56.2	1737	△ 6.11*	1044	693	664.3
66	71 06.4	38 59.4	1741	9.70	1659	82	673.3
67	71 06.3	39 02.6	1740	8.70	1488	252	683.9
68	71 06.3	39 05.7	1719	8.65*	1479	240	688.3
69	71 06.2	39 08.9	1743	8.47	1448	295	688.2
70	71 06.2	39 12.1	1747	9.00*	1539	208	688.3
71	71 06.1	39 15.3	1713	8.40*	1436	277	688.9
72	71 06.1	39 18.5	1733	8.82*	1508	225	692.3
73	71 06.0	39 21.6	1734	8.67*	1483	251	695.1
74	71 06.0	39 24.3	1733	7.38	1262	471	698.4
75	71 05.9	39 28.0	1749	8.70*	1488	261	698.7
76	71 05.9	39 31.2	1753	9.20*	1573	180	696.2
77	71 05.8	39 34.4	1751	8.55	1462	289	694.9
78	71 05.8	39 37.5	1757	8.47*	1448	309	696.9
79	71 05.8	39 40.7	1772	8.09	1383	389	696.2
80	• 71°05′40″	• 39°43′53″	1767	9.80*	1676	91	690.8
81	71 05.7	39 47.4	1767	9.33	1595	172	683.6
82	71 05.7	39 50.8	1775	11.25	1924	−149	677.7
83	71 05.8	39 54.1	1780	11.25	1924	−144	678.2
84	71 05.8	39 57.5	1793	9.74	1666	127	679.8
85	71 05.8	40 01.0	1794	9.90	1693	101	676.6
86	71 05.8	40 03.5	1799	△ 11.21*	1917	−118	672.3
87	71 05.8	40 06.8	1817	10.24	1751	66	669.6

Table 3. (Continued)

Station				Radio Echo Sounding			gravity value
No.	Latitude	Longitude	Elevation (m)	One-way echo time (μs)	Ice thickness (m)	Bedrock elevation (m)	go (mgal)
							982
C 88	71°05.8′S	40°10.2′E	1817	△ 7.11*	1215	602	663.4
89	71 05.8	40 13.6	1806	△ 7.00*	1197	609	657.6
90	71 05.8	40 17.1	1802	△ 7.05*	1206	596	660.8
91	71 05.8	40 20.5	1805	△ 10.16*	1737	68	668.1
92	71 05.8	40 23.9	1801	△ 11.37*	1944	−143	670.6
93	71 05.9	40 27.3	1787	9.67	1654	133	673.0
94	71 05.9	40 31.8	1794	10.50*	1796	− 2	674.1
95	71 05.9	40 35.3	1796	△ 8.53*	1764	32	673.2
96	71 05.9	40 38.7	1790	9.84	1683	107	679.7
97	71 05.9	40 42.0	1809	9.00	1539	270	684.8
98	71 06.0	40 45.5	1824	9.67	1654	170	678.2
99	71 06.0	40 48.9	1838	△ 9.89	1692	146	666.4
100	71 06.0	40 52.4	1823	11.50	1967	−144	664.3
101	71 06.0	40 55.7	1827	11.13	1903	− 76	665.1
102	71 06.0	40 59.1	1827	12.25	2095	−268	661.4
103	71 06.1	41 02.5	1838	△ 12.00	2052	−214	662.6
104	71 06.1	41 06.0	1837	11.63	1989	−152	664.9
105	71 06.1	41 09.5	1836	11.13	1903	− 67	667.1
106	71 06.1	41 12.8	1853	11.50	1967	−114	667.2
107	71 06.2	41 16.2	1856	△ 12.00	2052	−196	668.1
108	71 06.3	41 19.6	1860	10.25	1753	107	672.4
109	71 06.3	41 23.1	1875	10.70	1830	45	674.5
110	71 06.3	41 26.6	1889	10.67	1825	64	675.2
111	71 06.3	41 29.9	1890	11.13	1903	− 13	673.3
112	71 06.3	41 33.3	1889	11.75	2009	−120	671.3
113	71 06.4	41 36.7	1917	△ 12.53*	2142	−225	669.2
114	71 06.4	41 40.2	1934	△ 12.58*	2151	−217	664.5
115	71 06.4	41 43.6	1930	△ 6.63*	1134	796	660.1
116	71 06.5	41 47.0	1919	△ 8.63*	1476	443	658.9
117	71 06.5	41 50.4	1904	10.50	1796	108	664.0
118	71 06.6	41 53.8	1937	10.63	1818	119	671.4
119	71 06.6	41 57.3	1969	11.00	1881	88	671.1
120	71 06.6	42 00.7	1984	△ 11.58*	1980	4	665.5
121	71 05.6	42 03.1	1991	12.13	2074	− 83	664.5
122	71 05.3	42 05.4	1991	12.63	2160	−169	657.8
123	71 04.8	42 07.7	1993	7.89	1350	643	650.5
124	71 04.2	42 10.1	1982	△ 9.16*	1566	416	647.4
125	71 03.6	42 12.3	1968	△ 7.68*	1314	654	652.1
126	71 02.9	42 14.6	1958	△ 6.58*	1125	833	655.2
127	71 02.3	42 17.0	1963	△ 8.84*	1512	451	653.3
128	71 01.7	42 19.3	1965	△ 13.05*	2232	−267	649.6
129	71 01.1	42 21.5	1966	△ 14.42*	2466	−500	648.6
130	71 00.5	42 23.8	1978	13.63*	2331	−353	650.8
131	70 59.8	42 26.2	1985	13.75*	2351	−366	650.9
132	70 59.2	42 28.4	1994	12.50*	2138	−144	650.6
133	70 58.7	42 30.8	2004	△ 12.00*	2052	− 48	652.3
134	70 58.1	42 33.1	2003	△ 13.53*	2313	−310	656.8
135	70 57.4	42 35.4	1998	△ 13.32*	2277	−279	660.3

Table 3. (Continued)

Station				Radio Echo Sounding			gravity value
No.	Latitude	Longitude	Elevation (m)	One-way echo time (μs)	Ice thickness (m)	Bedrock elevation (m)	go (mgal)
							982
C136	70°56.8′ S	42°37.7′ E	1993	△ 13.58*	2322	−329	659.6
137	70 56.2	42 40.0	1988	△ 13.95*	2385	−397	658.9
138	70 55.6	42 42.4	1994	△ 13.26*	2268	−274	660.5
139	70 55.0	42 44.6	2000	△ 12.53	2142	−142	662.3
140	70 54.4	42 46.9	2002	△ 13.37	2286	−284	663.1
141	70 53.8	42 49.3	2006	△ 14.21*	2430	−424	665.2
142	70 53.1	42 51.5	2012	△ 12.21	2088	− 76	667.4
143	70 52.6	42 53.8	2016	—	—		668.4
144	70 52.0	42 56.2	2025	—	—		668.9
145	70 51.3	42 58.5	2031	—	—		670.0
146	70 50.7	43 00.8	2029	△ 7.74*	1323	706	670.5
147	70 50.1	43 03.1	2040	△ 12.42*	2124	− 84	669.5
148	70 49.8	43 05.6	2054	△ 8.21*	1404	650	667.2
149	70 49.8	43 08.3	2044	△ 8.63	1476	568	664.6
S 170	● 70°50′38″ S	● 43°11′32″ E	2034	11.50*	1967	67	669.8

Symbols explanation:

○ : Geodetic position by astronomic survey by JARE–9.

● : Geodetic position by astronomic survey by JARE–10.

(●): Geodetic positions of S240 and A075 were calculated by the triangulation chain from A001. These values agree well with those obtained by astronomic surveys at each station. Geodetic position of B48 was decided from an astronomic station at a nunatak, northeast of D massif of the Yamato Mountains.

□ : Geodetic position by the traverse of JARE-11.

△ : One-way echo time obtained by JARE-14.

* : The mark indicates that there are multi-echoes.

− : Negative sign means the bedrock surface is below the mean sea level.

Table 4. Geodetic positions of the station, surface elevation of ice sheet, ice thickness, and bedrock elevation along the inland traverse route of JARE-10.

Station No.	Distance (km)	Latitude	Longitude	Surface Elevation (m)	One-way Echo time (μ sec)	Ice Thickness (m)	Bedrock Elevation (m)	Remarks
0	0	69°02.0′S	39°43′E	21	—	—		
	1.3			69	1.25	214	−145	
	1.5				1.20	205		
A1	1.7	69 01.9	39 44	81	1.50	257	−176	
	1.9				1.20	205		
	2.2				1.00	171		
	2.4				1.50	257		
Y12	2.9	69 01.9	39 46	164	1.65	282	−118	
	3.4				1.90	325		
	3.7				1.65	282		
	3.9				1.30	222		
Y11	4.3	69 02.0	39 48	253	1.20	205	48	
	4.4				1.45	248		
	4.9				1.50	257		
	5.4				1.95	333		
Y10	5.6	69 02.1	39 49	290	2.00	342	−52	
	5.9				1.75	299		
	6.2				2.00	342		
	6.4				2.25	385		
Y 9	7.0	69 02.1	39 51	346	4.00	684	−338	
	7.4				3.80	650		
	7.5				4.10	701		
	7.7				4.50	770		
	7.9				4.90	838		
Y 8	8.0	69 02.2	39 52	360	4.90	838	−478	
	8.4				5.00	855		
Y 7	9.3	69 02.2	39 54	385	1.75	299	86	
	9.5				1.50	257		
	9.7				1.40	239		
	9.9				1.40	239		
	10.1				1.60	274		
	10.3				2.00	342		
	10.4				2.10	359		
	10.5				2.25	385		
Y 6	10.6	69 02.3	39 56	441	2.50	428	13	
	10.7				2.50	428		
	10.9				2.65	453		
P 3	11.1				2.65	453		
	11.4				2.70	462		
	11.7				2.90	496		
Y 5	12.0	69 02.3	39 57	471	2.65	453	18	
	12.2				2.55	436		
	12.4				2.50	428		
Y 4	12.7	69 02.3		496	2.60	445	51	
	12.9		39 59		3.00	513		
	13.2				2.25	385		
Y 3	13.7	69 02.3	40 01	519	2.30	393	126	
Y 2	13.9	69 02.3	40 01	534	2.85	487	47	
	14.2				2.80	479		

Table 4. (Continued)

Station No.	Distance (km)	Latitude	Longitude	Surface Elevation (m)	One-way Echo Time (μ sec)	Ice Thickness (m)	Bedrock Elevation (m)	Ramarks
P 4	14.4				2.75	470		
Y 1	14.9	69°02.3′S	40°01′E	539	2.75	470	69	
	15.2				2.40	410		
	15.5				2.60	445		
	15.8				2.50	428		
16	16.0	69 02.2	40 01	553	2.50	428	125	
	16.1				2.25	385		
	16.6				2.40	410		
	17.1				2.45	419		
17	17.6	69 01.9	40 04	583	2.45	419	164	
	18.1				2.50	428		
	18.6				2.90*	496		*2.50, 2.75
	19.1				2.70*	462		*2.60, 2.75
18	19.6	69 01.7	40 07	609	3.00	513	96	
	20.0				3.35	573		
	20.5				3.90	667		
	21.0				5.10	872		
19	21.5	69 01.5	40 10	634	6.60	1129	−495	
	22.1				7.20	1231		
	22.6				7.00	1197		
	23.1				6.10	1043		
20	23.6	69 01.5	40 12	653	5.60	958	−305	
	23.9				4.50	770		
	24.4				3.85	658		
	24.9				3.35	573		
21	25.4	69 01.6	40 15	699	3.10	530	169	
	25.9				3.50	599		
	26.4				3.90	667		
	26.9				4.70	804		
22	27.4	69 01.7	40 18	743	4.20	718	25	
	27.8				4.60	787		
	28.3				4.40	752		
	28.8				4.40	752		
23	29.3	69 01.8	40 21	771	4.30	735	36	
	29.7				4.00	684		
	30.2				4.00*	684		*3.80
	30.7				5.00*	855		*3.80
24	31.2	69 01.9	40 24	811	4.40*	752	59	*4.10
	31.6				4.80*	821		*4.10
	32.1				4.70	804		
	32.6				4.50*	770		*4.10
25	33.1	69 02.2	40 27	844	4.10	701	143	
	33.5				4.50	770		
	34.0				4.00	684		
	34.5				4.00	684		
26	35.0	69 02.3	40 29	870	4.20	718	152	
	35.9				4.40	752		
	36.4				4.30	735		
	36.9				5.00	855		
	37.0				4.80	821		

Table 4. (Continued)

Station No.	Distance (km)	Latitude	Longitude	Surface Elevation (m)	One-Way Echo Time (μ sec)	Ice Thickness (m)	Bedrock Elevation (m)	Remarks
27	37.2	69°02.5′S	40°32′E	893	5.50	941	−48	
	37.7				5.20	889		
	38.2				5.00	855		
	38.7				5.30	906		
28	39.2	69 02.7	40 35	916	5.60	958	−42	
	39.6				5.70	975		
	40.1				5.70	975		
	40.6				4.80	821		
29	41.1	69 02.8	40 38	935	5.00	855	80	
	41.6				5.00	855		
	42.1				5.00	855		
	42.6				5.20	889		
30	43.0	69 03.1	40 40	961	5.10	872	89	
	43.4				5.00	855		
	43.9				5.20	889		
	44.4				5.20	889		
31	44.9	69 03.3	40 43	981	5.70*	975	6	*5.20
	45.3				5.60	958		
	45.8				5.90	1009		
	46.3				6.40	1094		
32	46.8	69 03.6	40 46	994	6.50	1112	−118	
	47.2				6.00	1026		
	47.7				6.60	958		
	48.2				5.20	889		
33	48.7	69 03.9	40 48	1014	6.80*	1163	−149	*5.50
	49.0				5.80	992		
	49.5				6.60	1129		
	50.0				6.10	1043		
34	50.5	69 04.2	40 51	1030	6.00	1026	4	
	51.0				5.90	1009		
	51.5				6.00	1026		
	52.0				6.00	1026		
35	52.5	69 04.4	40 54	1046	6.60	1129	−83	
	52.9				6.50	1112		
	53.4				6.20	1060		
	53.9				6.10	1043		
36	54.4	69 04.8	40 56	1064	6.10	1043	21	
	54.9				6.20	1060		
	55.4				5.80	992		
	55.9				5.80	992		
37	56.4	69 04.8	40 59	1074	5.90	1009	65	
	56.8				5.80	992		
	57.3				6.40	1094		
	57.8				6.30	1077		
38	58.3	69 04.9	41 02	1088	6.20	1060	28	
	58.7				6.50	1112		
	59.2				6.50	1112		
	59.7				6.80	1163		
39	60.2	69 04.8	41 05	1099	7.00	1197	−98	
	60.6				7.20	1231		

Table 4. (Continued)

Station No.	Distance (km)	Latitude	Longitude	Surface Elevation (m)	One-way Echo Time (μ sec)	Ice Thickness (m)	Bedrock Elevation (m)	Remarks
	61.1				7.40	1265		
	61.6				6.30	1077		
40	62.1	69°04.7′S	41°07′E	1112	6.40	1094	18	
	62.5				6.50	1112		
	63.0				6.90	1180		
	63.5				6.50	1112		
41	64.0	69 04.6	41 10	1124	6.50	1112	12	
	64.4				6.30	1077		
	64.9				6.70	1146		
	65.4				6.40	1094		
42	65.9	69 04.6	41 13	1138	6.50	1112	26	
	66.3				6.50	1112		
	66.8				6.60	1129		
	67.3				6.60	1129		
43	67.8	69 04.5	41 15	1148	7.10*	1214	−66	*6.80
	68.2				6.60	1129		
	68.7				6.80	1163		
	69.2				7.00	1197		
44	69.7	69 04.3	41 18	1164	7.10	1214	−50	
	70.1				6.80	1163		
	70.6				6.60	1129		
	71.1				7.00	1197		
45	71.6	69 04.4	41 21	1179	6.90	1180	−1	
	72.0				6.90	1180		
	72.5				7.00	1197		
	73.0				6.80	1163		
46	73.5	69 04.5	41 24	1188	6.90	1180	8	
	74.0				7.00	1197		
	74.5				7.00	1197		
	75.0				7.00	1197		
47	75.5	69 04.3	41 26	1184	7.00	1197	−13	
	75.8				7.30	1248		
	76.3				7.10	1214		
	76.8				7.00	1197		
48	77.3	69 04.2	41 29	1200	7.10	1214	−14	
	77.8				7.20	1231		
	78.3				7.20	1231		
	78.8				6.80	1163		
49	79.3	69 04.2	41 32	1208	6.40	1094	114	
	79.7				6.40	1094		
	80.2				6.60	1129		
	80.7				7.00	1197		
50	81.2	69 04.2	41 35	1215	7.60	1300	−85	
	81.6				7.00	1197		
	82.1				6.90	1180		
	82.6				7.00	1197		
51	83.1	69 04.1	41 37	1217	7.60	1300	−83	*6.90
	83.5				6.90	1180		
	84.0				6.70	1146		
	84.5				6.80	1163		

Table 4. (Continued)

Station No.	Distance (km)	Latitude	Longitude	Surface Elevation (m)	One-Way Echo Time (μ sec)	Ice Thickness (m)	Bedrock Elevation (m)	Remarks
52	85.0	69°04.1′S	41°40′E	1227	7.10	1214	13	
	58.4				7.00	1197		
	85.9				7.00	1197		
	86.4				7.20	1231		
53	86.9	69 04.0	41 43	1233	7.10	1214	19	
	87.3				6.00	1026		
	87.8				6.00	1026		
	88.3				6.30	1077		
54	88.8	69 04.1	41 46	1259	6.60	1129	130	
	89.0				6.50	1112		
	89.5				6.50	1112		
	90.0				6.80	1163		
55	90.5	69 04.2	41 48	1271	7.00	1197	74	
	90.9				6.90	1180		
	91.4				6.60	1129		
	91.9				6.80	1163		
56	92.4	69 03.7	41 51	1274	6.80	1163	111	
	92.9				6.80	1163		
	93.4				6.40	1180		
	93.9				6.30	1077		
57	94.4	69 03.8	41 54	1276	7.20*	1231	45	*6.90
	94.8				6.00	1026		
	95.3				6.00	1026		
	95.8				5.60	958		
58	96.3	69 04.2	41 57	1287	5.50	941	346	
	96.7				5.50	941		
	97.2				5.90	1009		
	97.7				6.00	1026		
59	98.2	69 04.4	41 59	1307	6.20	1060	247	
	98.6				6.60	1129		
	99.1				6.60	1129		
	199.6				6.60	1129		
60	100.1	69 04.6	42 02	1332	7.70	1317	15	
	00.6				8.10	1385		
	101.0				8.20	1402		
	101.5				8.80	1505		
61	102.0	69 05.0	42 04	1335	7.90	1351	−16	
	102.4				7.80	1334		
	102.9				8.30	1419		
	103.4				8.70	1488		*8.20
62	103.9	69 05.2	42 07	1341	8.20	1402	−61	
	104.3				8.20	1402		
	104.8				8.50	1454		
	105.3				8.50	1454		
63	105.8	69 05.3	42 09	1348	8.40	1436	−88	
	106.3				8.40	1436		
	106.8				8.40	1436		
	107.3				8.40	1436		
64	107.8	69 05.5	42 12	1356	8.70	1488	−132	
	108.2				8.70	1488		

Table 4. (Continued)

Station No.	Distance (km)	Latitude	Longitude	Surface Elevation (m)	One-way Echo Time (μ sec)	Ice Thickness (m)	Bedrock Elevation (m)	Remarks
	108.7				9.00*	1539		*8.20
	109.2				8.10	1385		
65	109.7	69°05.8′ S	42°15′ E	1362	8.00	1368	−6	
	110.1				7.20	1231		
	110.6				6.90	1180		
	111.1				6.90	1180		
66	111.6	69 05.9	42 18	1366	7.00	1197	169	
	112.0				7.00	1197		
	112.5				7.40*	1265		*6.90
	113.0				7.20	1231		
67	113.5	69 06.0	42 21	1363	7.80*	1334	29	*6.80
	113.9				7.60*	1300		*6.60
	114.1				6.60	1129		
	114.5				6.50	1112		
	115.0				6.80	1163		
68	115.3	69 06.2	42 23	1380	7.20	1231	149	
	115.5				8.00	1368		
	116.1				8.00	1368		
69	117.3	69 06.4	42 26	1381	8.40*	1436	−55	*7.40
	117.8				7.40	1265		
70	119.1	69 06.9	42 29	1388	8.00	1368	20	

Note: Distance was measured by distance meter of snow-car. Multi-echoes (*) are shown in remarks.

Table 5. Geodetic position of the station, surface elevation of ice sheet, ice thickness and bedrock elevation along the traverse route of JARE-10, around the Yamato Mountains.

Station No.	Distance (km)	Latitude	Longitude	Ice Surface Elevation (m)	One-Way Echo Time (μ sec)	Ice Thickness (m)	Bedrock Elevation (m)	Remarks
B 1	0	71°48.8′ S	36°11′ E	2242	2.35*	402	1840	2.10
2	1.0	71 48.7	36 10	2224	2.63	449	1775	
	2.0				3.60	616		
3	3.0	71 47.4	36 07	2217	6.04*	1033	1184	5.80
4	5.0	71 46.5	36 05	2202	5.24	896	1306	
	6.0				4.80	821		
5	6.5	71 46.0	36 04	2182	5.20*	889	1293	4.70
	7.5				5.40	923		
6	9.0	71 45.4	36 00	2170	4.20	718	1452	
7	10.0	71 45.3	35 58	2156	3.65	624	1532	
8	11.0	71 45.0	35 57	2144	3.63*	620	1524	3.10
	12.0				2.50*	428		2.00
9	13.0	71 44.6	35 54	2143	1.90	375	1768	
10	20.0	71 44.4	35 51	2157	—	—	—	
11	21.3	71 44.0	35 49	2122	—	—	—	
12	23.5	71 44.0	35 47	1991	2.05	351	1640	
	23.7				2.45*	419		1.80, 2.13
	24.2				3.30	564		
	25.2				2.70	462		
13	25.6	71 43.4	35 42	1933	2.95	504	1429	
	26.9				5.00	855		
	27.9				4.84*	828		4.50
14	29.1	71 41.7	35 40	1918	4.60*	787	1131	3.85, 4.10
	30.1				3.85	658		
	31.1				5.30	906		
15	32.2	71 40.5	35 37	1888	4.25*	727	1161	4.00
	33.2				6.70	1146		
16	34.2	71 39.5	35 35	1877	7.13	1218	659	
	35.2				6.50	1112		
17	36.2	71 38.6	35 33	1857	5.75*	983	874	5.90
18	37.2	71 38.4	35 31	1847	5.73	979	868	
	38.2				9.00*	1539		6.00
19	39.2	71 37.4	35 30	1819	8.83*	1510	309	5.20
	40.2				5.50*	941		4.00, 4.60
20	41.1	71 36.4	35 30	1800	5.30*	906	894	5.00
	42.1				4.00	684		
21	43.0	71 37.4	35 30	1793	3.83*	654	1139	3.50
	44.0				4.00*	684		3.50
22	45.0	71 34.1	35 30	1765	6.00*	1026	739	5.60
	45.8				5.60	958		
23	46.8	71 33.0	35 30	1750	5.36*	917	833	5.04, 5.20
	47.8				5.50	941		
24	48.8	71 32.0	35 29	1740	4.48	765	975	
	49.8				2.73	466		
25	50.5	71 31.0	35 29	1724	2.50	428	1296	
	51.5				2.65	453		
26	52.6	71 30.4	35 27	1713	3.43	586	1127	
	53.6				5.00	855		
27	54.5	71 29.5	35 24	1705	5.00*	855	850	4.40

Table 5. (Continued)

Station No.	Distance (km)	Latitude	Longitude	Ice Surface Elevation (m)	One-way Echo Time (μ sec)	Ice Thickness (m)	Bedrock Elevation (m)	Remarks
	55.5				5.50	941		
B28	56.5	71°29.0′S	35°22′E	1704	5.80	992	712	
	59.1				7.60	1300		
	59.6				7.50*	1283		6.80
29	61.5	71 28.5	35 19	1705	6.88*	1257	448	6.08, 6.53
								7.35
30	62.2	71 27.5	35 21	1718	7.40*	1265	453	3.20, 4.50
	63.2				3.00	513		
	63.7				5.04*	862		4.50, 4.00
31	64.2	71 26.6	35 22	1700	6.00*	1026	674	5.50
	64.7				6.60*	1129		5.70
	65.2				6.06	1036		
32	66.1	71 26.0	35 20	1694	5.90	1009	685	
	67.1				7.05*	1206		5.60, 6.32
33	68.1	71 25.1	35 21	1680	4.80	821	859	
	68.7				4.90	838		
	69.2				5.70	975		
34	70.1	71 24.5	35 22	1663	5.20	889	774	
	71.1				5.60*	958		4.13, 5.03
35	72.1	71 23.5	35 24	1649	5.00	855	794	
	72.9				5.10	872		
	73.1				5.64	964		
36	74.0	71 22.6	35 25	1635	7.00*	1197	438	5.00
	75.0				8.00*	1368		4.75
37	75.4	71 22.0	35 25	1632	6.70	1146	486	
	80.1				6.10	1043		
	80.5				—	—	—	
38	82.8	71 21.4	35 23	1643	—	—	—	
39	84.8	71 20.5	35 22	1638	—	—	—	
40	85.8	71 19.5	35 21	1641	—	—	—	
41	87.7	71 20.0	35 24	1630	5.00	855	775	
	88.7				3.60	616		3.60
42	89.6	71 20.5	35 26	1647	5.30*	906	741	
	90.0				4.50	770		
	90.6				6.20	1060		7.00
	93.9				7.80*	1334		
43	94.5	71 20.0	35 29	1671	7.30	1248	423	
	95.5				7.00	1197		5.05
44	96.5	71 20.1	35 32	1671	7.80*	1334	337	5.00
	97.5				8.60*	1471		
45	98.5	71 20.5	35 36	1685	8.33	1424	261	9.30
	99.5				10.50*	1796		10.20, 9.40
								7.88
46	100.5	71 21.0	35 39	1705	11.12*	1901	−196	8.40
	101.5				9.20*	1573		
	102.5				9.00	1539		9.83, 8.33
47	103.5	71 22.1	35 39	1743	11.33*	1937	−194	9.10
	104.5				10.60*	1813		
	105.2				5.13	876		5.60
48	106.3	71 23.0	35 41	1800	6.50*	1112	688	4.00

Table 5. (Continued)

Station No.	Distance (km)	Latitude	Longitude	Ice Surface Elevation (m)	One-Way Echo Time (μ sec)	Ice Thickness (m)	Bedrock Elevation (m)	Remarks
	107.3				5.00*	855		3.50
	108.1				5.50*	941		3.15
C001	108.9	71°23.6′ S	35°44.6′ E	1813	4.60*	787	1026	
	109.6				4.35	744		
	110.2				4.50	770		
002	111.2	71 21.9	35 48.1	1832	3.68	628	1204	
	112.2				4.58	782		
	113.0				6.50	1112		
003	113.2	71 21.4	35 50.9	1848	6.40*	1094	754	5.95
	114.2				3.80	650		
004	115.2	71 20.8	35 53.7	1828	4.83*	825	1003	4.50
	116.2				5.30	906		
005	117.1	71 20.4	35 56.5	1808	4.70*	804	1004	4.33, 3.55
	118.3				6.20	1060		
006	119.1	71 19.7	35 59.3	1796	6.53	1116	680	
007	121.0	71 19.3	36 02.1	1794	(8.00)	(1368)	(426)	
008	123.0	71 18.7	36 04.9	1790	(9.11)	(1557)	(233)	
009	124.9	71 18.2	36 07.8	1779	(7.16)	(1224)	(555)	
010	126.8	71 17.6	36 10.5	1768	6.85	1171	597	
	127.8				6.80	1163		
011	128.8	71 17.2	36 13.2	1764	8.15*	1394	370	7.40
	129.8				7.50	1283		
012	130.8	71 16.5	36 16.0	1757	7.50*	1283	474	7.15
	131.8				7.00	1197		6.50
013	132.7	71 16.1	36 18.8	1754	7.35*	1257	497	5.84, 5.60
	133.7				6.30*	1077		5.00
014	134.6	71 15.5	36 21.6	1758	6.75	1154	604	
	135.6				6.00	1026		
015	136.6	71 15.0	36 24.4	1763	8.35*	1428	335	7.43
	137.6				7.90	1351		
016	138.5	71 14.4	36 27.2	1759	7.50	1283	476	
	139.5				7.20	1231		
017	140.2	71 13.9	36 30.0	1759	7.25	1240	519	

Note: Distance was measured by distance meter of snow-car. Multi-echoes (*) are shown in remarks.